Chromatography-Mass Spectrometry-Based Identification of Triterpenes and Phenolic Compounds in Maskwio'mi (*Betula papyrifera* Marshall Bark Extract)

by Volodymyra Zuieva

A thesis submitted to the School of Graduate Studies in partial fulfillment of the requirements

for the degree of

Master of Science

Department of Chemistry

Memorial University of Newfoundland

May 2025

St. John's, Newfoundland and Labrador, Canada

Abstract

Maskwio`mi is a traditional topical treatment used by the Mi`kmaq people to treat a variety of skin conditions, including eczema and psoriasis. It is typically obtained through the pyrolysis of *Betula papyrifera* Marshall (paper birch) bark via a can-over-can method. To replicate those conditions under controlled settings, a pyrolysis reactor system developed by Dr. Bierenstiel was used to recreate the production of maskwio`mi in the laboratory. The resulting bio-oil, also referred to as an extract, is formed of a complex mixture, containing hundreds of organic compounds, which makes it challenging to characterize. Chromatography coupled with mass spectrometry is the common technique used for bio- oil composition analysis. This approach has been applied to *Betula* species analysis, which led to the identification and subsequent isolation of bioactive compounds, including triterpenoids and phenolic compounds. Although some of these compounds can have therapeutic effects, certain phenolic compounds, such as cresols, are recognized as environmental pollutants due to their toxicity and potentially harmful effect on humans and animals, which necessitates their accurate identification and quantification in bio-oil samples.

This thesis presents the identification and quantification of phenolic compounds and lupane-type triterpenes. First, the concentrations of *ortho*-, *meta*-, and *para*-cresol were found to be from 324 to 1,240 mg/L using a full-scan GC-MS method. Selected reaction monitoring (SRM) was employed to quantify nine compounds, which ranged from 192 to 5,909 mg/L. Furthermore, betulin and betulinic acid were quantified at concentrations of 2,411 ± 45 ppm and 199 ± 8 ppm using a UHPLC-MS method.

Acknowledgements

I would like to express my gratitude to everyone who supported me during this journey. First of all, I want to thank my supervisor, Dr. Matthias Bierenstiel, who enabled my Master's in Canada and contributed to my attending various conferences. Secondly, I would like to acknowledge my committee members, Dr. Christina Bottaro and Dr. Stephanie MacQuarrie, for their support and effort even during busy times. Both have been excellent examples of women in STEM, whose dedication and leadership I admire.

A very special thank you goes to Dr. Raj Kalia, who taught me how to use various instruments and spent countless hours helping me. Beyond that, he shared the invaluable lesson of maintaining a positive mindset through every challenge. I extend my heartfelt appreciation to Aderonke Oludare, Trisha Ang, and Karen Foss, whose wisdom and friendship taught me so much.

I would also like to thank my parents as well as other members of Cape Breton University who were supportive during these two years.

Table of Contents

Table of Figures

List of Tables

List of Abbreviations and Symbols

Da	Dalton
°C	degree Celsius
°C/min	degree Celsius per minute
eV	electronvolt
kPa	kilopascal
min	minutes
mg/L	milligrams per liter
m	meters
mm	millimeters
µm	micrometers
µL	microliters
m/z	mass-to-charge ratio
s	seconds
%	percent
wt%	weight percent
ACN	acetonitrile
APCI	atmospheric pressure chemical ionization
APPI	atmospheric pressure photoionization
BEH	ethylene bridged hybrid
BSTFA	*N*,*O*-*bis*(trimethylsilyl)trifluoroacetamide
$C_6H_5^+$	phenyl cation
$C_6H_7^+$	arenium ion

$C_7H_6^+$	tropylium cation
CHO	aldehyde group
EI	electron ionization
ESI	electrospray ionization
FID	flame ionization detector
FTIR	Fourier transform infrared spectroscopy
GC	gas chromatography
GC-MS	gas chromatography-mass spectrometry
GC-MS/t-SRM	time-dependent selected reaction monitoring-based gas chromatography-mass spectrometry
HTC	hydrothermal carbonization
H_2O	water
L-DOPA	levorotatory isomer of 3,4-dihydroxyphenylalanine
LC	liquid chromatography
LC-MS	liquid chromatography-mass spectrometry
LOD	limit of detection
LOQ	limit of quantification
MS	mass spectrometry
MTBSTFA	*N*-tert-Butyldimethylsilyl-*N*-methyltrifluoroacetamide
OH	hydroxyl group
QTOF	quadrupole time of flight
RSD	relative standard deviation
R^2	correlation coefficient

SC-CO_2	supercritical carbon dioxide
SIM	selected ion monitoring
SRM	selected reaction monitoring
TBDMS	tert-butyldimethylsilyl chloride
TMS	tetramethylsilane
UHPLC	ultra-high performance liquid chromatography
UHPLC-MS	ultra-high performance liquid chromatography-mass spectrometry
UHPLC-QTOF-MS	ultra-high performance liquid chromatography-quadrupole time-of-flight mass spectrometry

Chapter 1. Introduction

1.1 Natural products in drug discovery

Natural products are bioactive compounds derived from plants, animals, or microorganisms and have been essential to medicine for centuries.[1] Traditional medicines around the globe, like traditional Chinese medicine, Ayurveda, and indigenous healing, have applied the therapeutic potential of nature to treat illnesses, forming a basis for many modern pharmaceuticals.[2] As of 2018, approximately 67% of anticancer drugs originated from natural products.[3] For instance, paclitaxel (Taxol), a chemotherapy drug derived from the Pacific yew tree (*Taxus brevifolia*) is one of the most used anti-cancer therapeutics (Figure 1.1).[4] Additionally, another yew species, native to the Central Himalayas, *T. baccata*, has been used in traditional medicine for cancer treatment.[4] Another great example of nature-derived medicine, artemisinin, represents the class of anti-malarial drugs derived from extracts of sweet wormwood (*Artemisia annua*), which is a traditional Chinese medicine.[5]

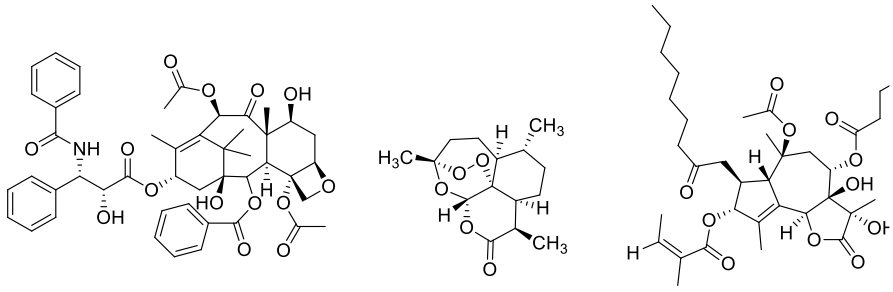

Figure 1.1. Examples of drugs originating from nature.[4]

Multiple extensive reviews by Newman and co-workers highlight the ongoing importance of natural products in modern drug discovery.[6–9] For the period of 1989 to 1995, 60% of antimicrobial and anticancer drugs were reported to originate from natural sources.[6] In 2003, despite the productivity crisis of pharmaceutical companies due to multiple industry challenges, the demand for diversity-oriented libraries of natural product-like compounds has risen.[10,11] Therefore, there is a necessity to expand the research, especially due to the ongoing loss of biodiversity.[7]

Over the last decade, interest in natural products and their diverse bioactivity has increased significantly, particularly in extracts and essential oils. For instance, Lee and Hyun have reported the rising demand for plant materials and their extracts in the cosmetic industry.[12] Cuanalo-Contreras and Moreno-Gonzalez reported the same trend for the pharmaceutical sector, where natural products are getting recognition for various conditions, including neurodegenerative diseases.[13] Considering their structural diversity and evolutionary bioactivity, natural products remain a crucial source for developing new medicines.

1.2 Bioactive compounds in *Betula species*

The genus *Betula*, also known as birch, has been used in traditional medicine in various cultures due to its therapeutic properties. In southeast Europe, the extract of european silver birch (*Betula pendula* Roth) leaves is traditionally utilized for the treatment of rheumatic diseases and blood purification, indicating anti-inflammation activity.[14,15] Similarly, Himalayan silver birch (*Betula utilis*) bark has also been reported for the treatment of

rheumatism, wound healing, and skin conditions.[16] Among indigenous tribes along the Missouri River, river birch (*Betula nigra*) leaves were applied to treat skin ailments.[17]

Research on extracts of various parts of *Betula species* has led to the isolation of bioactive compounds, including triterpenoids, flavonoids, and other phytochemicals.[18] Triterpenes, particularly lupane-type compounds like betulin and betulinic acid, are among the most studied classes of compounds derived from *Betula species* (Figure 1.2 A). These compounds have been reported to possess various pharmacological properties, such as anti-microbial, anti-inflammatory, anti-cancer, and other biological activities.[19,20] For instance, Ghimire and co-workers stated that *Betula alnoides* bark extract exhibits anti-microbial and anti-inflammatory activities attributed to the presence of phytochemicals, which include betulin and other triterpenes.[21] Betulin is a crucial secondary metabolite predominantly found in the bark of *Betula species*, however, the concentration varies on the species.[22] Dehelean and co-workers reported that betulin forms up to 24.5 wt% of dried silver birch (*Betula verrucosa)* outer bark.[23] O'Connell and co-workers identified this natural product at 6.8 wt%, 11.9 wt%, and 17.6 wt% for heartleaf birch (*Betula cordifolia*), paper birch (*Betula papyrifera*), and gray birch (*Betula populifolia*), respectively. However, the highest concentration was found in yellow birch (*Betula alleghaniensis*), which contains up to 56% of betulin.[24] Dehelean and co-workers suggest that betulin has antitumor potential as betulin-enriched birch bark extracts have shown significant cytotoxic effects on cancer cell lines. [23]

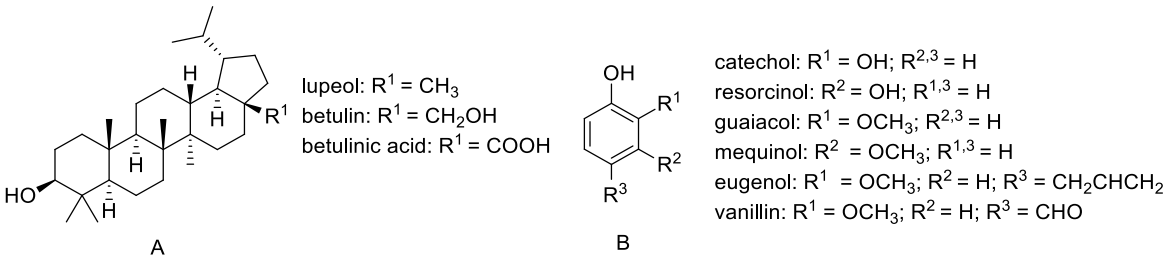

Figure 1.2. (A) Chemical structures of selected lupane-type triterpenes and (B) phenolic compounds.

Betulinic acid is another bioactive compound derived from the bark of the *Betula species*. Numerous studies have been conducted to identify and characterize betulinic acid, attributable to its promising therapeutic activity, which includes anticancer, antimicrobial, and anti-inflammatory properties. Drenkhan and co-workers confirmed the presence of betulinic acid alongside betulin while conducting a comparative analysis of bioactive compounds in *Betula pendula*.[19] Additionally, Szoka and co-workers reported that betulinic acid demonstrates significant antineoplastic activity in human digestive system cancer cells.[25]

Phenolic compounds, another valuable class of phytochemicals, are characterized by one or multiple hydroxyl functional groups attached to an aromatic ring (Figure 1.2 B). These compounds are widely abundant in plants, particularly teas, fruits, vegetables, and tobacco.[26] Phenols are generally recognized for their antioxidant activity [27] due to the ability to scavenge free radicals. Amongst the most well-studied phenolic compounds are flavonoids and tocopherols reported to exhibit a variety of biological actions, including antioxidant, antiviral, and anti-inflammatory.[28,29]

Methoxyphenols, a less-known subclass of phenolic compounds, are characterized by one or more methoxy groups on an aromatic ring. These guaiacyl-type compounds often originate from the thermal degradation of lignin, a natural polymer abundant in the cell walls of wood.[30] For instance, *Betula species*, including *Betula papyrifera,* are rich in lignin and, consequently, in methoxyphenols, such as guaiacol, eugenol, and vanillin. These compounds, typically generated *in situ* and released during the pyrolysis of birch wood and bark, indicate that the *Betula genus* is a valuable source of phytochemicals. Methoxyphenols garnered attention due to their potential bioactivity, which includes antioxidant, anti-inflammatory, and antimicrobial properties.

Benzenediols, or catechols, are another class of phenolic compounds and are widely used in pharmaceuticals. For instance, catechol derivatives are intermediates for the synthesis of *L*-3,4-dihydroxyphenylalanine (*L*-DOPA), which is used for Parkinson's disease treatment.[31] Resorcinol, another benzenediol, is utilized in low doses in topical treatments for its keratolytic and antiseptic activity.[32]

Despite having beneficial properties, the use of phenols is strictly regulated due to their cytotoxicity and potential skin irritation, which necessitates the quantification of phenolic compounds.

Overall, an extensive analysis of *Betula papyrifera* extract is crucial to explore its full potential as a source for drug discovery.

1.3 Lignocellulose biomass

Biomass refers to organic material derived from plants, animal waste, or algae.[33] Lignocellulosic biomass is the most abundant biochemical on the planet, which includes mainly forestry and agricultural waste. Forestry biomass can be divided into two groups, softwood and hardwood.[34] *Betula genus* is classified as hardwood, which comes from angiosperm plants. Hardwood is characterized by large water-conducting pores surrounded by fibrous cells.[35]

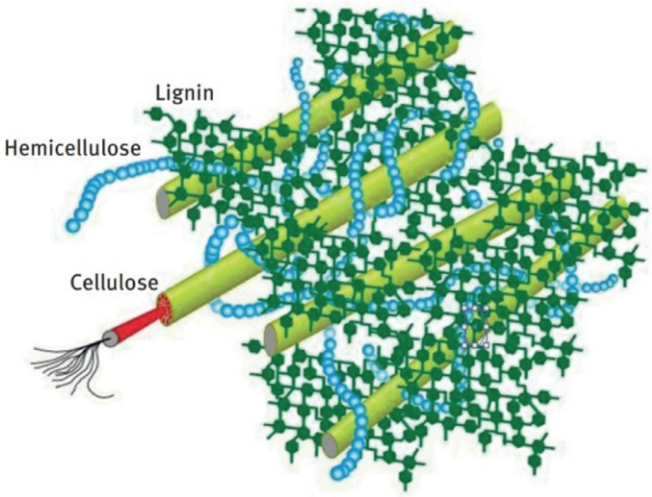

Figure 1.3. Constituents of lignocellulosic biomass.[33]

Lignocellulosic biomass consists of several key components: cellulose, hemicellulose, lignin, extractives, and ash (Figure 1.3).[36] In the cell wall, cellulose forms a tough skeletal framework with microfibers, while hemicellulose and lignin fill the inner spaces as linking materials.[33] Cellulose connects to hemicellulose and lignin mainly via hydrogen bonds, whereas hemicellulose and lignin form hydrogen and covalent bonds.[37] These tight

interactions create lignin-carbohydrate complexes, often leaving residual fragments of one in extracted samples of the other.[36]

The composition of each component depends on the type of biomass, typically ranging from 40 – 60% for cellulose, 15 – 30% for hemicellulose, and 10 – 25% for lignin. Particularly for *Betula papyrifera*, the cellulose content was reported to be approximately 44%,[38] while hemicellulose and lignin were 25% and 19.6%, respectively.[38,39]

1.4 Pyrolysis of biomass materials

Pyrolysis is a thermochemical process of biomass decomposition, generally around 300 °C to 700 °C, in the absence of oxygen.[40] During the pyrolysis of wood, numerous fractions are formed, solid (biochar), liquid (bio-oil), and gaseous (biogas), each comprised of various compounds. The relative proportion and composition of each fraction depends on the specific type of biomass used and pyrolytic conditions such as temperature, heating rate, and residence time.[40]

Biochar, also referred to as char, is a solid residue remaining after the pyrolysis of biomass, consisting of carbon-rich material and inorganic ash.[41] The content of biochar depends on the origin of the feedstock and operating conditions, typically making up 15 – 25 wt% of the products.[42] It is characterized by high porosity, low volatility and good electrical conductivity.[43] Biochar has a variety of applications, from use as a solid fuel, in soil remediation, carbon sequestration and as an electrode modifier.[42,43]

The biogas composition is highly dependent on the feedstock type and pyrolysis conditions.[42] It generally contains gases like carbon monoxide, carbon dioxide, hydrogen, methane, ethane, and ethene, along with traces of higher molecular weight gaseous organic compounds and water vapor.[44]

Bio-oil is a highly oxygenated liquid derived from pyrolysis.[40] It is also called pyrolysis oil, bio-crude oil, etc., however, in this study, the term 'extract' is used. Bio-oil is a dark-coloured, viscous liquid that forms a complex mixture of up to 300 organic compounds, typically with 30 – 40 wt% oxygen content, depending on the biomass feedstock and operating process.[42] These compounds could be classified as follows: acids (e.g., formic acid, acetic acid), carbonyl and hydroxycarbonyl products (e.g., hydroxyaldehydes, hydroxyketones), anhydrous sugars, phenols, and other aromatic compounds.[40,45]

Pyrolysis can be classified by several factors, including heating rate and residence time, temperature, process type, reactor type, method of heating, feedstock, etc. The simplest distinction is based on pyrolytic conditions. Fast pyrolysis involves high heating rates (10 – 200 °C/s), and short vapor residence time (0.5 – 10 s), typically occurring at temperatures around 450 to 550 °C (Table 1.1). The bio-oil is the primary product of this process (60 – 75 wt%), along with biochar (15 – 25 wt%) and syngas (10 – 20 wt%).[40] During slow pyrolysis, biomass is heated at much slower rates (0.1 – 2 °C/s) at temperatures ranging from 300 to 700 °C.[46] The yields of products are highly dependent on the exact conditions. The process tends to favor biochar production at lower temperatures and longer residual time.[47] Flash pyrolysis, also called ultra-fast pyrolysis, occurs at extremely high rates (10^3 – 10^4 °C/s) and residence time of less than 1 s. This predominantly forms bio-oil (60 – 75 wt%) due to the reduced impact of secondary combustion reactions during the

process.[48] Pyrolysis conducted at temperatures below 300 °C is usually referred to as torrefaction. It is usually characterized by a low heating rate (0.2 – 0.8 °C/s) and a vapor residence time of less than 30 min.

Table 1.1. Classification of pyrolysis types and characteristics.

Pyrolysis type	**Residence time**	**Heating Rate (°C/s)**	**Temperature (°C)**	**Main products**	**References**
Fast pyrolysis	0.5 – 10 s	High 10 – 200	450 – 550	Bio-oil (≤80 wt%)	[46,49]
Slow pyrolysis	10 – 60 min	Slow 0.1 – 2	300 – 750	Biochar, bio-oil, biogas (proportions depend on conditions)	[46,50,51]
Flash pyrolysis	0.1 – 0.5 s	Extremely high 10^3 – 10^4	350 – 550	Bio-oil (60 – 75 wt%)	[46,52,53]
Torrefaction	< 30 min	Slow 0.2 – 0.8	200 – 300	Biochar, bio-oil, biogas (proportions depend on conditions)	[44,54,55]

The heterogeneous nature of biomass makes it difficult to define a universal pyrolysis mechanism. Instead, pyrolysis includes various thermal degradation processes, typically proceeding through the following stages: moisture evaporation; depolymerization and volatilization; sustained degradation with char formation and occurrence of secondary and tertiary reactions.[42] Challenges for precise mechanistic studies arise from the intricate kinetics of simultaneous reactions and the formation of secondary products through interactions among pyrolysis intermediates and biomass molecules. Understanding the

primary thermal degradation mechanisms is crucial to optimizing the process and maximizing the yield of the preferred products. For example, Pakdel and co-workers studied betulin extraction by vacuum pyrolysis of *Betula papyrifera* bark at temperatures ranging from 250 to 300 °C under 0.7 kPa in a bench-scale reactor, followed by the recovery of extractives using dry ice-limonene condensers. Although the increase in temperature has led to a higher yield of products, no noticeable increase in betulin extraction was found.[56] In another study, birch twigs were pyrolyzed at 550 °C under a nitrogen atmosphere in a thermostated ceramic tube reactor. The analysis of the products by GC/FTIR/FID and GC/MS revealed a significant amount of carbon monoxide and carbon dioxide, along with methane being the predominant hydrocarbon. Various oxygenated organic compounds were also identified among the pyrolysates.[57] This highlights the importance of ongoing research on the pyrolysis of *Betula species*, aiming to reveal the full potential of this lignocellulosic biomass.

1.5 Maskwio`mi

Maskwio`mi is a traditional topical treatment used by the Mi`kmaq (L`nu) people.[58] It was obtained by the pyrolysis of *Betula papyrifera* bark, using a can-over-can method (Figure 1.4). This method will be reported in Chapter 5. After extracting, oil or extract was typically mixed with animal fat before application. This treatment could be used to treat a variety of skin issues such as eczema, psoriasis, etc.[59]

Figure 1.4. Traditional can-over-can method of obtaining maskwio`mi.

However, this method poses several challenges, including difficulties in temperature control, variability in yield, and overall low production. Moreover, as the process is conducted outdoors, it is susceptible to environmental fluctuations. Therefore, an electrical extractor (Figure 1.5) was designed to address these challenges and replicate the can-over-can method under controlled settings.

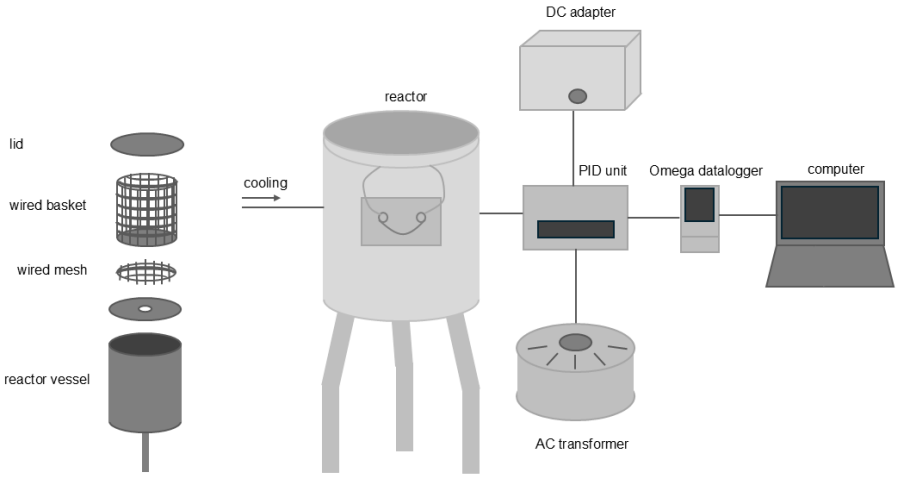

Figure 1.5. Schematic diagram of a pyrolysis reactor system.

The methodology and pyrolytic conditions for the reactor system are reported in Section 2.4.2.

1.6 Chromatographic methods coupled with mass spectrometry

1.6.1 Gas chromatography-mass spectrometry (GC-MS)

Gas chromatography with detection by mass spectrometry (GC-MS) is the common technique used for bio-oil composition analysis mainly due to the great separation efficiency, good sensitivity, and wide availability.[60,61] However, the complex composition of bio-oils poses challenges, such as insufficient resolution and peak coelution.[62] Gas chromatography separates based on their differences in boiling points and their partition between a gaseous mobile phase, typically helium, and a stationary phase coated inside a column. GC-MS is usually limited to volatile and non-polar compounds, hence, prior derivatization is required for polar and thermolabile compounds.[60,63] Non-polar (5%- phenyl)-methylpolysiloxane columns are the most commonly used for bio-oil analysis (Table 1.2). Low/mid-polarity and polar columns, coated with 14%-cyanopropyl-phenyl)-methylpolysiloxane and modified polyethylene glycol are used, though less frequently. The length of the columns varies, typically, the longer columns provide better resolution as they have a greater number of theoretical plates and better peak capacities.[63]

Table 1.2. GC-MS conditions for various feedstock.

Feedstock	Column	Heating profile	Reference
Wood (Pine)	DB-5 (30 m × 0.32 mm × 0.25 μm)	40 °C (4 min hold) → at 5 °C/min to 280 °C (15 min hold)	[64]
	DB-FFAP (30 m × 0.25 mm × 0.25 μm)	50 °C (5 min hold) → at 3 °C/min to 240 °C	[65]
Wood chips (Pine)	HP-5 (30 m × 0.32 mm × 0.25 μm)	35 °C (15 min hold) → at 4 °C/min to 310 °C	[66]
Sawdust (Pine)	DB-5 (60 m × 0.32 mm × 0.25 μm)	40 °C → 3 °C/min to 120 °C → at 2 °C/min 200 °C → at 10 °C/min to 280 °C (5 min hold)	[67]
	Restek-5Sil MS (30 m × 0.25 mm × 0.25 μm)	40 °C (4 min hold) → at 2.5 °C/min to 80 °C → at 4 °C/min to 250 °C → 10°C/min to 310 °C (10 min)	[68]
	DB-5 (60 m × 0.25 mm × 0.25 μm)	40 °C → at 3 °C/min to 300 °C	[69]
Wood (Oak)	DB-5 (30 m × 0.32 mm × 0.25 μm)	40 °C (4 min hold) → at 5 °C/min to 280 °C (15 min hold)	[64]
Wood (Beech)	DB-1701 (60 m × 0.25 mm × 0.25 μm)	45 °C → at 3 °C/min to 235 °C (13 min hold)	[70]
Husk (Rice)	HP-5MS (30 m × 0.32 mm × 0.25 μm)	60 °C → at 5 °C/min to 150 °C → at 7 °C/min to 300 °C	[71]
	OV-5 (30 m × 0.32 mm × 0.25 μm)	40 °C (2 min hold) → at 5 °C/min to 280 °C (10 min hold)	[72]

After separation, the sample is transferred to the ion source to be ionized, commonly using electron ionization (EI). In EI (Figure 1.6), electrons are emitted by a heated filament and accelerated to 70 eV, where the de Broglie wavelength of the electrons matches the bond length of most organic molecules, thus maximizing the possibility of ionization and fragmentation. By applying a small magnetic field parallel to the path of the electrons, they

are forced into a helical trajectory, increasing interaction time with sample molecules. The resulting molecular ions are then repelled into the accelerating region and directed into the mass analyzer at a fixed kinetic energy.

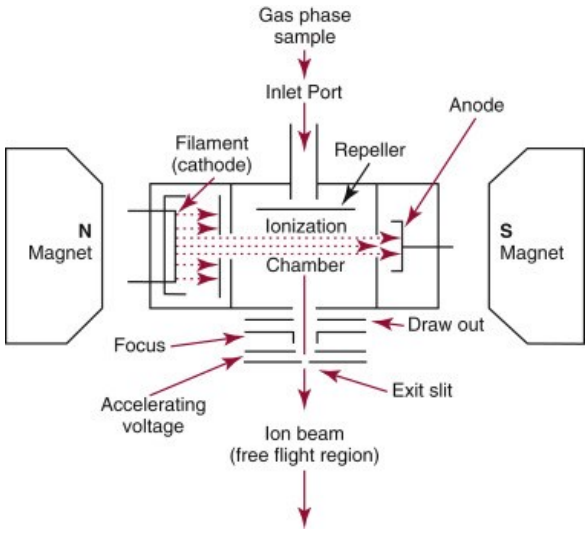

Figure 1.6. Scheme of the electron ionization source.[73]

In the mass analyzer, ions are separated based on their mass-to-charge ratio (*m/z*). The most commonly used analyzer in bio-oil analysis is the low-mass resolution single quadrupole (Figure 1.7). A quadrupole mass spectrometer or quadrupole mass filter consists of four parallel metal rods arranged symmetrically around a central z-axis. Two opposite rods experience an AC and a positive DC voltage, while the other two receive an AC and a negative DC voltage. A combination of DC and RF potentials influences the trajectory of the ions, so only a specific ion would maintain a stable path through the quadrupole and reach the detector, while others would become unstable and be filtered out.[63] Quadrupole-based systems offer robustness, high sensitivity and a good linearity range but can be limited in resolving power and mass accuracy compared to high-resolution-based systems, e.g. Orbitrap, FTICR.[60]

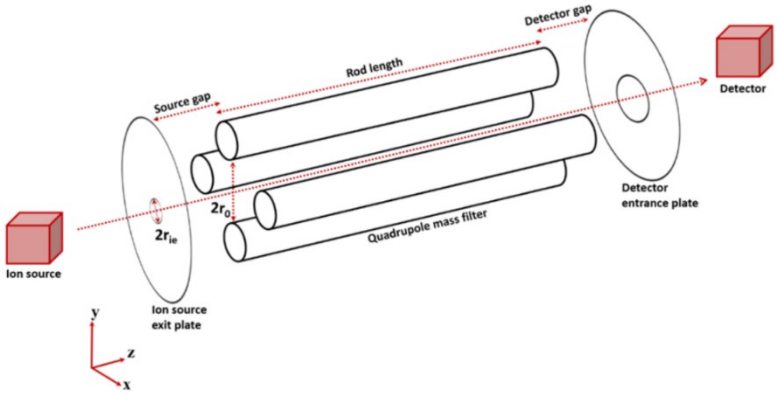

Figure 1.7. Scheme of quadrupole mass filter. [74]

Several studies have investigated bio-oil composition using GC-MS with quadrupole analyzers. Ingram and co-workers found levoglucosan to be the main component in both pine and oak bio-oils despite differences in hemicellulose content.[64] Furfuran derivatives and other carbohydrate-derived compounds made up to 25% of the total bio-oil composition. Dos Santos and co-workers developed a SIM-based GC-MS method to quantify 49 compounds out of 126 detected in five pine wood sawdust bio-oil samples.[69] Hydrocarbons, phenols, and benzofurans were found to be the predominant compounds. Similarly, Joseph and co-workers reported a bio-oil composition consisting of phenolics, furans, polyols, aldehydes, and carbohydrates but also identified resins and substituted stilbenes.[68] Aging studies showed that certain furan-ring sugars disappeared while hemicellulose-derived sugars emerged, possibly due to the aging-induced release of lignin-carbohydrate oligomers. GC-MS analysis with TMS derivatization contributed to 16% of the mass loss observed during aging.

Additionally, to reduce the complexity of the matrix, pre-fractionation methods, such as solvent extraction, have also been developed. However, the selectivity is not achieved,

resulting in a few fractions with varying polarities.[65] In one approach, five fractions were obtained by sequentially extracting the resulting rice husk bio-oil in a separatory funnel using n-hexane, tetrachloromethane, carbon disulfide, benzene, and DCM.[71] 167 organic compounds were identified by comparing the obtained mass spectra with NIST databases. Those compounds were classified into alkanes, alcohols, aldehydes, ketones, acids, esters, benzene, and nitrogen derivatives (Figure 1.8). The study also traced the origin of the products based on the biomass composition. Cellulose primarily degrades into alcohols, ketones, aliphatic acids, and esters, while hemicellulose produces similar compounds, along with furfurals. Lignin breaks down into aldehydes, aromatic acids, and esters, and in combination with extractives and proteins, it also forms amides, amines, and other nitrogen-containing compounds. Additionally, waxes degrade into alkanes.

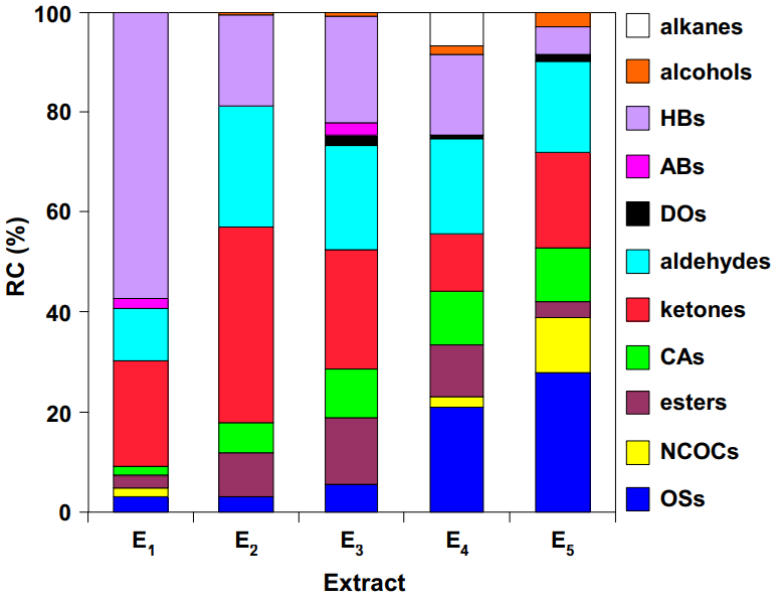

Figure 1.8. Different group components detected in E_1–E_5.[71]

Another pre-separation method, supercritical fluid extraction with CO_2, was developed as an attempt for selective fractionation of bio-oils. A sequential SC-CO_2 extraction on pine

wood bio-oil was performed in three steps: 5 min with pure CO_2, 25 min with 90% CO_2 / 10% methanol, and 40 min with 75% CO_2 / 25% methanol. GC-MS analysis identified 132 compounds out of 200 peaks detected by comparing retention time and mass spectra to the NIST library. SFE enabled the detection of 27 additional low-abundant compounds not found in raw bio-oil due to matrix effects. Semi-quantitative analysis revealed that carbohydrates, phenols, and ketones were the most abundant, with phenols being selectively enriched in the first fraction, while carbohydrates were in the second and third fractions (Figure 1.9).

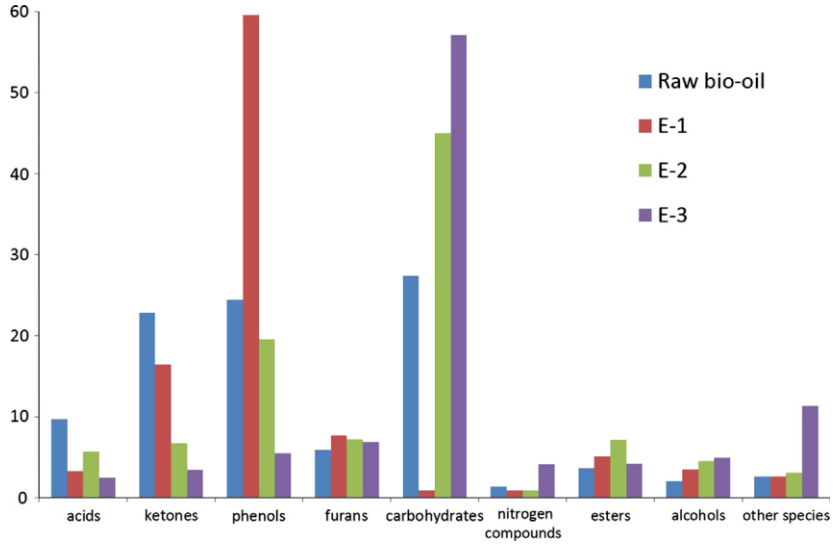

Figure 1.9. Relative abundance of various compound types identified in the bio-oil and its fractions by GC–MS.[65]

1.6.2 Pyrolysis-gas chromatography-mass spectrometry (PyGC-MS)

PyGC-MS is a chromatographic technique that integrates the thermal decomposition of biomass with the structural analysis of resulting pyrolytic products. Two configurations (online and offline) are typically used. In the online configuration, the products are directly transferred from the pyrolysis unit to the gas chromatograph. However, the setup has

several disadvantages, such as the inefficient detection of high-molecular compounds, poor separation of polar compounds, and the potential deterioration of GC columns.[61] In PyGC- MS (Table 1.3), the most frequently utilized columns are mid-polar columns coated with (14%-cyanopropyl-phenyl)-methylpolysiloxane, which are suitable for semivolatile compound analysis. For instance, Alsbou and Helleur demonstrated using a ZB-1701 column for enhancing peak separation.[75] The study showed that 47-56% of bio-oil samples from birch and pine wood were analyzed by PyGC-MS, exceeding the 40% detection efficiency by the conventional GC.

Table 1.3. PyGC-MS conditions for various feedstock.

Feedstock	**Column**	**Heating profile**	**Reference**
lignin	DB-1701 (60 m × 0.25 mm × 0.25 μm)	45°C (4 min) → at 3 °C/min to 280°C (15 min)	[76]
	VF-1701 (30 m × 0.25 mm × 0.25 μm)	40°C (5 min) → at 5 °C/min to 250°C (10 min)	[77]
Pine wood	Rtx-1707 (60 m × 0.25 mm × 0.25 μm)	40°C (3 min) → at 5 °C/min to 280°C (1 min)	[78]
	ZB-1701 (30 m × 0.25 mm × 0.25 μm)	35°C (6 min) → at 6 °C/min to 240°C (4 min)	[75]
Mesquite wood	Elite-1701 (30 m × 0.25 mm × 0.25 μm)	45°C (1 min) → at 5 °C/min to 275°C (3 min)	[79]
Birch wood	ZB-1701 (30 m × 0.25 mm × 0.25 μm)	35°C (6 min) → at 6 °C/min to 240°C (4 min)	[75]
sugarcane straw	DB-5 (30 m × 0.25 mm × 0.25 μm)	60°C (1 min) → at 4 °C/min to 280°C (15 min)	[80]

1.6.3 Liquid chromatography-mass spectrometry (LC-MS)

Liquid chromatography (LC) is another technique for bio-oil characterization. However, it is typically utilized either with other independent methods (e.g. FTIR, NMR) or coupled to a high-resolution mass analyzer. While LC offers lower separation efficiency compared to GC, it allows the analysis of a wider range of analytes, including volatile, non-volatile, polar, and thermolabile compounds. Despite its versatility, the analysis of heavy bio-oil fractions, e.g. polymers derived from cellulose and lignin degradation, might not be possible, which could be attributed to the irresistible adsorption of highly polar compounds.[81]

HPLC is the most used form of LC, where separation occurs based on the distribution of analytes between a liquid mobile phase (solvent) and a stationary phase (column coating). The retention of compounds depends on their affinity for these phases.[82] According to Table 1.4, reverse-phase chromatography (RP-HPLC) is a widely used method characterized by a non-polar stationary phase (typically C18) and a polar mobile phase (water, methanol, acetonitrile). In contrast to normal-phase chromatography, non-polar compounds are retained longer in RP-HPLC due to their stronger interaction with the stationary phase.

Table 1.4. LC-MS conditions for various feedstock.

Feedstock	Column	Solvent A/B; elution	Ionization	Analyzer	Reference
Birch bark	Syncronis 50 × 2.1 mm C18 1.7 µm	ACN/H_2O; gradient	ESI	Orbitrap	[83]
Birch wood chips	ACQUITY UPLC BEH 50 × 2.1 mm C18 1.7 µm	H_2O/ACN; gradient	ESI	Quadrupole	[84]
Wood pellets	Syncronis C18 (50 mm × 2.1 mm × 1.7 µm)	ACN/H_2O; gradient	ESI	Orbitrap	[85]
Ligno-cellulosic biomass	Kinetex C18 2.6 µm particles 100 × 3 mm	H_2O/MeOH; gradient	ESI, APCI	FTICR	[86]
Pine sawdust	C18 (150 mm × 75 µm × 5 µm)	H_2O/ACN; gradient	ESI	QTOF	[68]

Efficient ionization is essential for the accurate identification of bio-oil components. However, due to the complex composition of bio-oil, different compounds exhibit varying ionization efficiencies, and thus, no single technique can ionize all compounds without competition effects.[61] Therefore, a combination of ionization techniques with different selectivity is often required.[87]

Electrospray ionization (ESI) is the most used ionization for bio-oil characterization using HPLC-MS. In ESI (Figure 1.10), a dilute analyte solution is transferred through a metal capillary at a low flow rate (1 – 20 µL/min).[88] A high voltage (2 – 6 kV) applied to the capillary tip generates a strong electric field, dispersing the solution into charged droplets. A coaxial sheath gas (nitrogen) helps nebulization and directs the spray toward

the mass spectrometer. Solvent evaporation reduces the size of the droplets until free analyte ions are released. The ions pass through a sampling cone or heated capillary (100 – 300 °C) into the high vacuum of the mass spectrometer, while the heated capillary ensures complete desolvation.

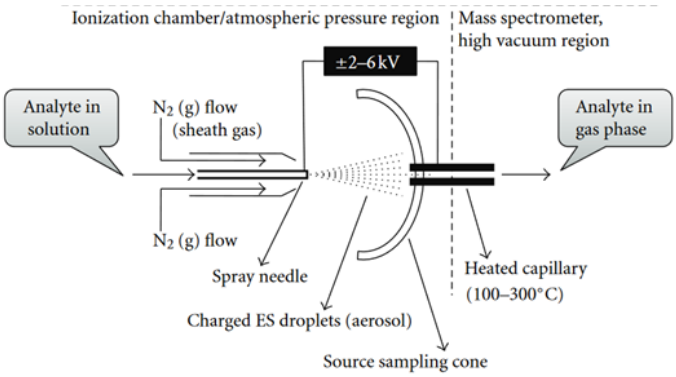

Figure 1.10. Scheme of an ESI source.[88]

ESI is best suited for polar to highly polar compounds and is particularly effective for thermally unstable species.[89] Most oxygenated compounds in bio-oil are protic and readily deprotonated, therefore, negative ESI mode is preferred,[90] while positive ESI mode is used for aprotic and basic compounds.[91] Yet, the efficiency of ESI can be influenced by dopants and pH. For instance, Smith and co-workers found that the pH significantly affected signal intensity in negative ESI mode, while ammonium formate and other organic modifiers impacted ionization efficiency.[92] Similarly, Hertzog and co-workers observed that nitrogen-containing compounds showed stronger signals when doped with ammonium acetate or formic acid in positive ESI mode.[91]

APCI is another ionization technique used in HPLC-MS. In APCI (Figure 1.11), a sample is sprayed into the ionization chamber through a capillary and is nebulized by a

high-speed nitrogen beam, forming small droplets.[93] Then, they enter a heated vaporization chamber, where they undergo desolvation and convert into a gas-phase molecular mist. Ionization occurs when a corona discharge needle applies a high voltage, generating reactant ions that interact with the analytes and lead to the formation of protonated molecular ions in positive mode and anion attachment or electron capture in negative mode.

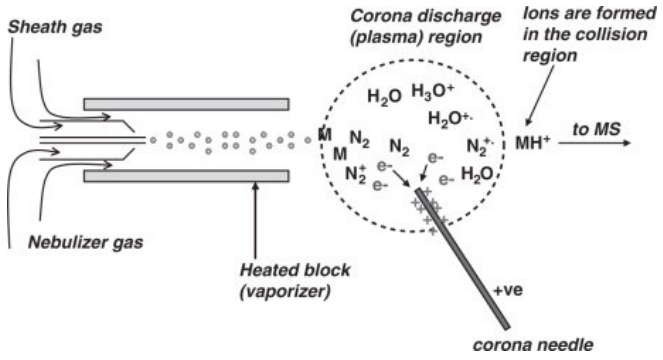

Figure 1.11. Scheme of atmospheric pressure chemical ionization source.[94]

APCI is effective for low to moderate polarity compounds with molecular masses up to 1500 Da.[93] However, unlike ESI, APCI requires some volatility and thermal stability of the analyzed compounds.[61]

Various mass analyzers coupled to LC have been utilized for bio-oil characterization (Table 1.4), which includes quadrupole mass filter, quadrupole time-of-flight (QTOF), Orbitrap, and Fourier transform ion cyclotron resonance (FTICR). The principles of the quadrupole mass spectrometer were discussed earlier in the chapter. An example of LC- Q- MS could be the study by Meile and co-workers that reported the identification of several compounds, such as furfural, vanillin, syringol, levoglucosan, glucose, and xylose, using SIM-based ultra-high performance liquid chromatography (UHPLC)-ESI-MS.[84]

The QTOF mass spectrometer is a hybrid that combines the two techniques, consisting of three quadrupoles, including a pre-filter quadrupole and a time-of-flight tube (Figure 1.12). The quadrupole Q0 is an ion guide that allows the low-pressure gases coming from LC to be pumped away and focus the ions prior to the transmission to the next quadrupole. Q1 functions as a mass filter, allowing only ions of a specific mass to pass through. The third quadrupole Q2 is a collision cell, where, under the appropriate RF applied, ions undergo collision-induced dissociation (CID) by interacting with argon molecules bled into the source. The fragmented ions are reaccelerated into the ion modulator region, where an electric field pulses the ions, accelerating them orthogonally to their original trajectory. Then, they enter the reflectron, which compensates for minor velocity differences and extends the path of the ions by forcing them to reverse direction, improving mass resolution. Finally, the ions reach the microchannel plate (MCP) detector, where they are amplified and detected. QTOF exhibits excellent mass accuracy, fast acquisition speed, and theoretically unlimited mass range, despite its limitation in quantitative performance and dynamic range.[93,95] As an example, Joseph and co-workers used a Q-TOF LC-MS/MS system to analyze bio-oil aging products and identified over 1000 distinct chromatographic peaks.[68] By peracetylating the samples, the ionization efficiency and chromatographic separation of polar and high-molecular-weight compounds were improved.

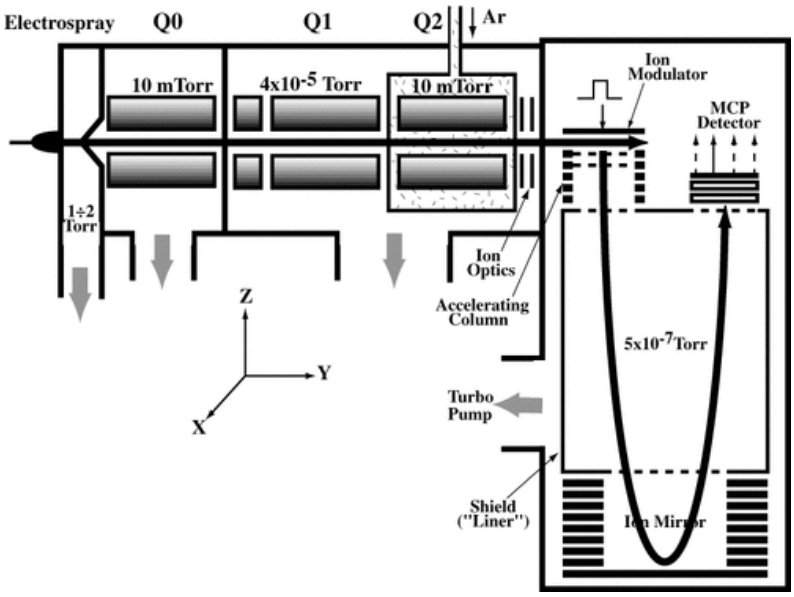

Figure 1.12. Scheme of QTOF.[96]

High-resolution mass spectrometry (HRMS) is a highly sensitive technique used in bio-oil analysis for untargeted analysis. In contrast to low- and mid-resolution analyzers like single quadrupoles and TOF, HRMS instruments such as Orbitrap and FT-ICR MS achieve resolutions exceeding 100,000.[97] For instance, a comparison of Q-TOF MS and FT-ICR MS was conducted for the characterization of eucalyptus bio-oil.[98] At *m/z* 351 (Figure 1.13), FT-ICR MS (400,000) resolved six distinct compounds, in comparison Q- TOF MS (resolution 5,000) detected only one, thus unable to resolve two closely spaced ions. However, even though Q-TOF is not able to perform a comprehensive analysis of bio-oils, it could still detect major compounds while being cheaper and more robust.

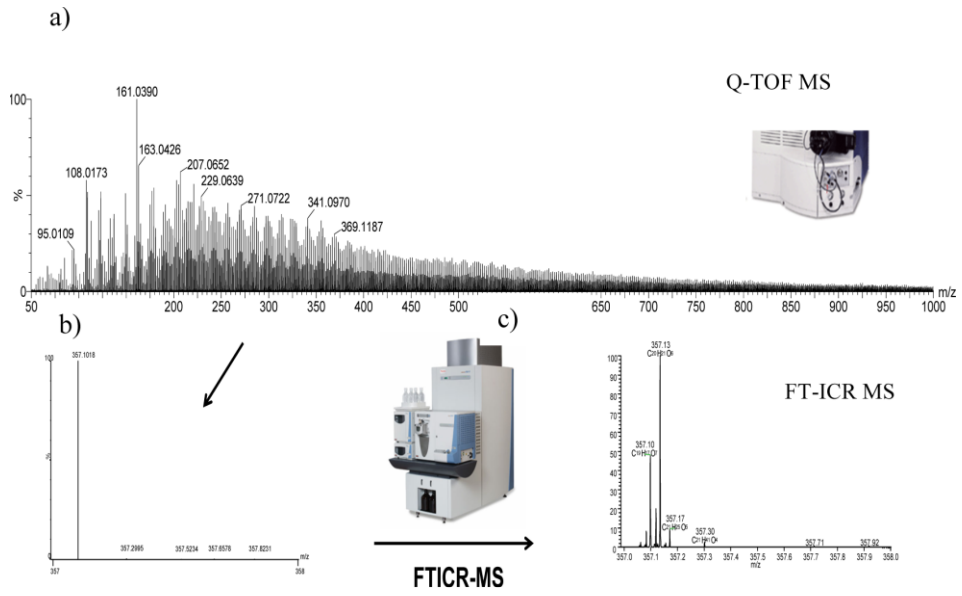

Figure 1. 13. (A) ESI spectrum of eucalyptus bio-oil using Q-TOF MS. *m/z* from 351.00 to 351.40 using (B) Q-TOF MS (resolution of 5000) and (C) FT-ICR MS (resolution of 400 000).[98]

1.7 Thesis Objectives

The characterization of pyrolysis-derived products, especially bio-oil, poses a challenge due to the complexity of the matrix. As mentioned previously, pyrolysis produces a mixture of hundreds of compounds, each presenting in low concentrations. This complexity results in overlapping peaks in the chromatographic separation, making it challenging to resolve individual components. The solubility issue further complicates the characterization, which can be addressed by sample preparation.

Thus, the objective of this thesis is to address the discussed challenges and to provide insights into the chemical composition of *Betula papyrifera* extract. This will involve targeted and untargeted analyses using combined chromatographic and mass spectrometric

techniques, along with further quantification of bioactive compounds (phenolic and triterpene. I conducted all the experiments and prepared the drafts of this thesis.

Chapter 2. Identification of cresol isomers using GC-MS

2.1 Introduction

Pyrolysis is a thermochemical process of converting biomass into char, bio-oil and gas products in the absence of oxygen. This process is commonly applied to lignocellulosic biomass which primarily consists of cellulose, hemicellulose, and lignin.[36] While thermal degradation of cellulose and hemicellulose yields sugars and light volatiles, depolymerization of lignin results in the formation of various phenolic compounds. In the case of hardwood, the primary products of lignin degradation are syringol, guaiacol, and their derivatives, including cresols [56] as shown in Figure 2.1.

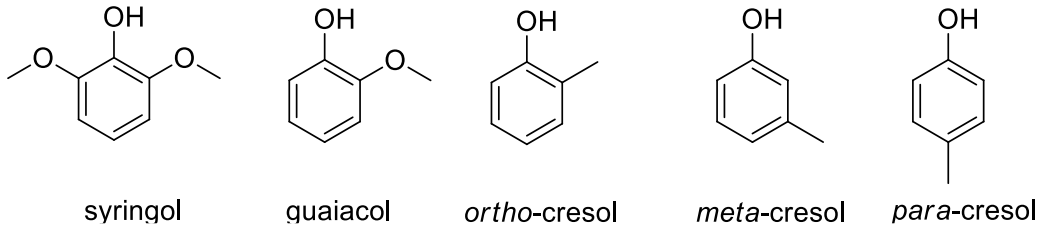

Figure 2.1. Structures of several phenolic compounds as the main phenolic compounds obtained in the pyrolysis of lignin.

Cresols are recognized as environmental pollutants due to their toxicity and potential effect on humans and animals.[99] However, due to the lack of information on their carcinogenicity,[100] they were not classified as human carcinogens, according to the American Conference of Governmental Industrial Hygienists (ACGIH) and International Agency for Research on Cancer (IARC).[101,102] 2.3 to 5 ppm was established as the exposure limit for phenol and cresol isomers.[101]

The majority of analysis methods for cresols identification require derivatization due to the tendency of hydrogen bond formation, which leads to low volatility and affects sensitivity in GC.[103] Derivatization is achieved by transformation procedures including alkylation, acylation or silylation of the phenolic OH group into aryl alkyl ethers, esters and aryl silicates. In the case of cresols, silylation agents, *N*-tert-butyldimethylsilyl-*N*-methyltrifluoroacetamide (MTBSTFA) and *N*,*O*-*bis*(trimethylsilyl)trifluoroacetamide (BSTFA), are typically utilized to transfer a TBDMS or TMS onto the phenol group and making it less hydrophilic.[104] Schummer and co-workers suggested that MTBSTFA should be preferred over BSTFA for its higher analytical response in GC-MS.[105] Typically, ultrasound-assisted or microwave-assisted extraction is performed prior to sample preparation, followed by solid-phase extraction.[106] Another study reported solid-liquid extraction with low-temperature purification and cresol derivatization using BSTFA with further selected ion monitoring-based GC-MS method.[107]

This chapter reports the quantification of cresols without prior derivatization. This study aimed to develop an easy and efficient method to quantify cresols in the birch bark extract.[108]

2.2 Results and discussion

2.2.1 Gas chromatographic separation of cresol isomers

This study aimed to develop an easy and efficient method to quantify cresols in the birch bark extract without a derivatization step. The identification was performed using full scan data acquisition mode on a gas chromatograph instrument coupled with a low-polarity

column. Rtx-5MS column, coated with 5% diphenyl-95% dimethylpolysiloxane, was selected for chromatographic separation as it allows the analysis of both polar and non-polar compounds. Initially, a three-step temperature program with a total of 30 min run was developed for the isomer identification. The oven temperature was kept at 50 °C for 1.0 min, ramped to 200 °C at 10.0 °C /min with a hold time of 5.0 min, then ramped again to 280 °C at 15.0 °C /min with a hold time of 5.0 min. The run time was later shortened to a two-step 15-minute programming with the temperature kept at 50 °C for 1.0 min, then ramped to 200 °C at 10.0 °C/min with a hold of 5.0 min. The chromatograms of cresol standards are shown in Figures 2.2-2.5. *Ortho*-cresol signal occurred at 5.204 min while *meta*-cresol and *para*-cresol eluted at 5.345 and 5.338 min, respectively, confirmed by control experiments with pure compounds as reference. The elution of the cresol isomers correlates with a lower boiling point of *ortho*-cresol, at ambient pressure, of 191.0 °C, while *meta*- and *para*-isomers have very close boiling points of 202.2 °C and 201.9 °C.[109]

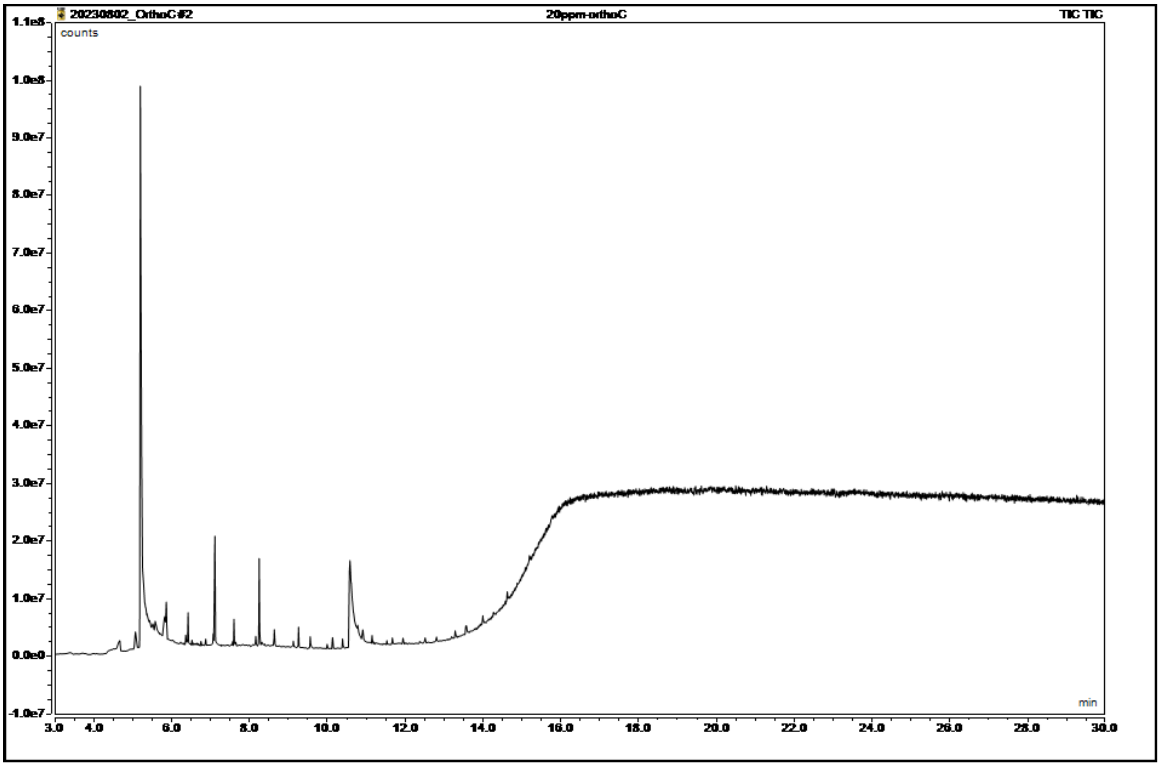

Figure 2.2. Analysis of 20 mg/L of ortho-cresol eluting at 5.204 min. Total run of 30 min on Thermo Scientific Trace 1310 Gas Chromatograph equipped with a Restek Rtx-5MS column and TSQ 9000.

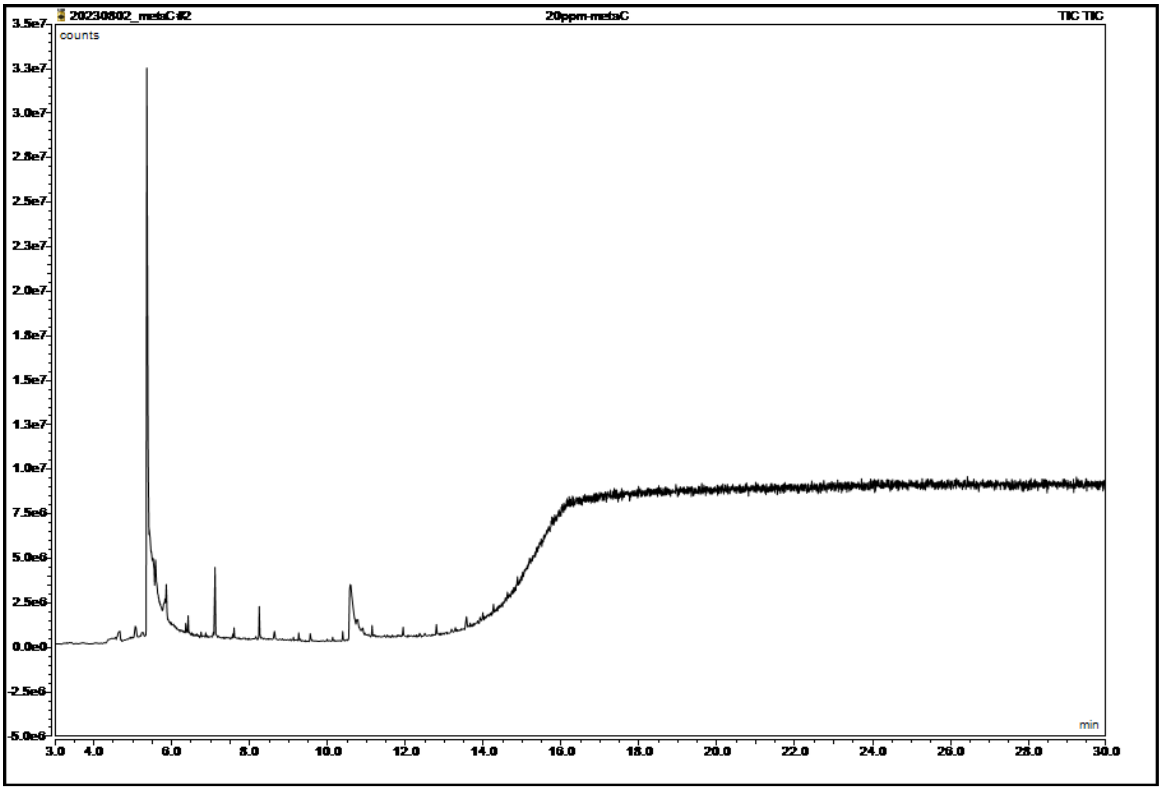

Figure 2.3. Analysis of 20 mg/L of meta-cresol eluting at 5.345 min. Total run of 30 min on Thermo Scientific Trace 1310 Gas Chromatograph equipped with a Restek Rtx-5MS column and TSQ 9000.

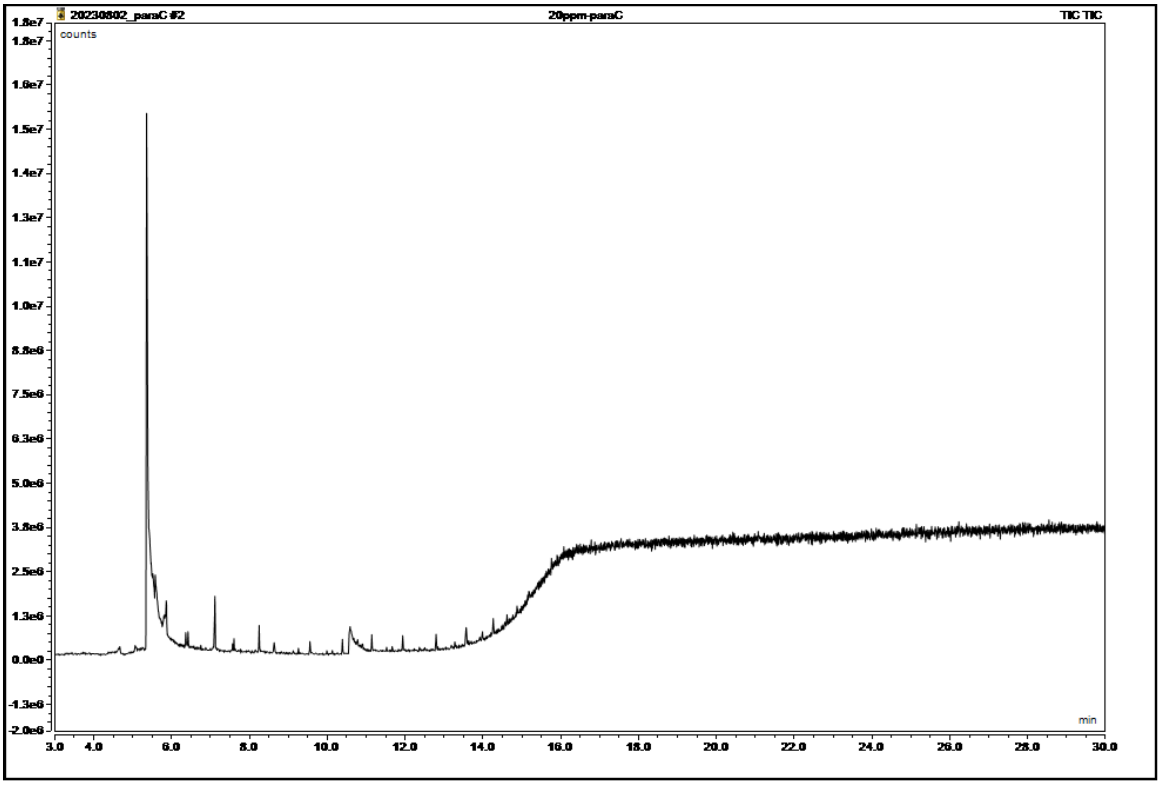

Figure 2.4. Analysis of 20 mg/L of para-cresol eluting at 5.338 min. Total run of 30 min on Thermo Scientific Trace 1310 Gas Chromatograph equipped with a Restek Rtx-5MS column and TSQ 9000.

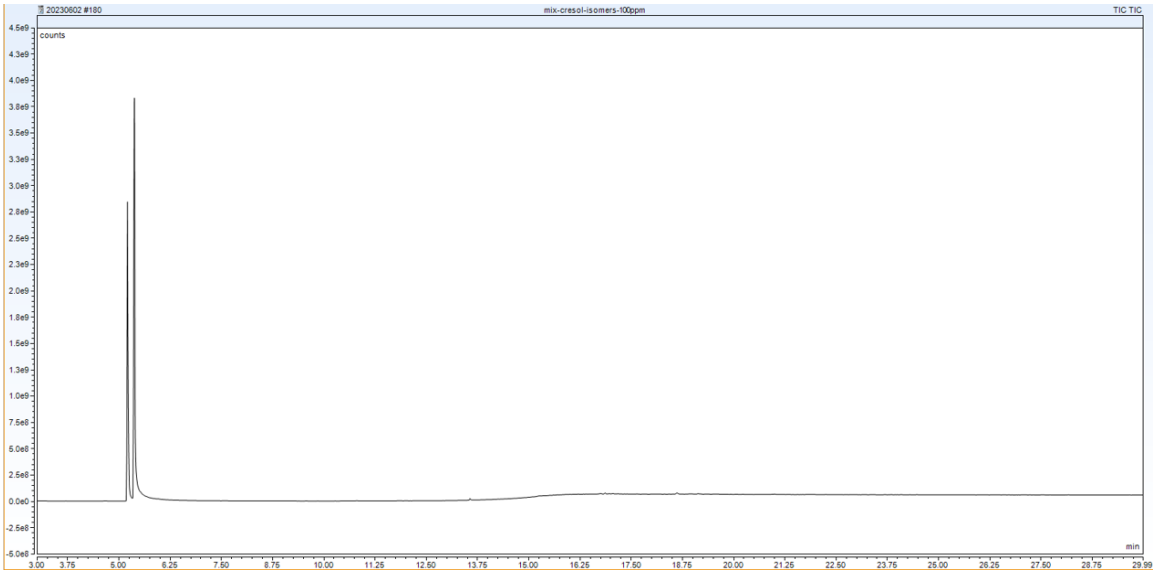

Figure 2.5. Analysis of 100 mg/L mix of cresol isomers. Ortho-cresol elutes at 5.204 min, while meta- and para-isomers elute together at 3.355 min. Total run of 30 min on Thermo Scientific Trace 1310 Gas Chromatograph equipped with a Restek Rtx-5MS column and TSQ 9000.

Analytes underwent fragmentation by electron ionization at 70 eV with a triple quadrupole MS detector. The mass spectra of isomers were obtained in the range of 50 to 550 Da with an optimal dwell time of 0.2 s (Figures 2.6-2.8). The base peak at *m/z* 108.1 corresponds to the molecular ion $[M]^{+\cdot}$ of *ortho*-cresol, followed by the fragment at *m/z* 107.1 by loss of proton. The first fragmentation pathway involves the loss of H_2O, producing the fragmentation ion $C_7H_6^+$ at *m/z* 90. Another fragmentation pathway attributed to the loss of CHO resulted in the fragmentation ion $C_6H_7^+$ at *m/z* 79. Further fragmentation reaction forms a phenyl intermediate $C_6H_5^+$ at *m/z* 77.

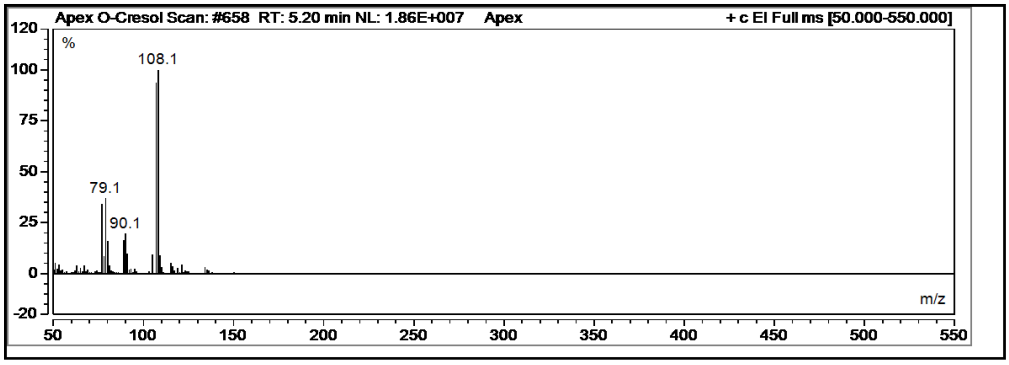

Figure 2.6. Mass spectrum of ortho-cresol. Base peak at m/z 108.1 on Thermo Scientific Trace 1310 Gas Chromatograph equipped with a Restek Rtx-5MS column and TSQ 9000.

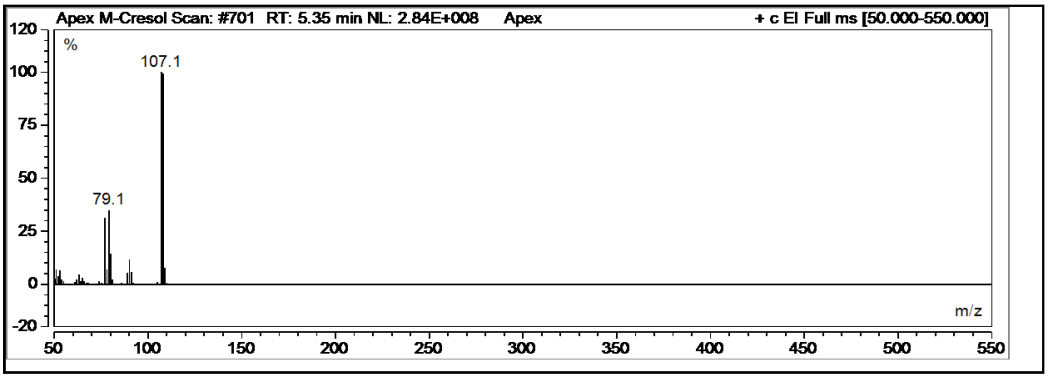

Figure 2.7. Mass spectrum of meta-cresol. Base peak at m/z 108.1 on Thermo Scientific Trace 1310 Gas Chromatograph equipped with a Restek Rtx-5MS column and TSQ 9000.

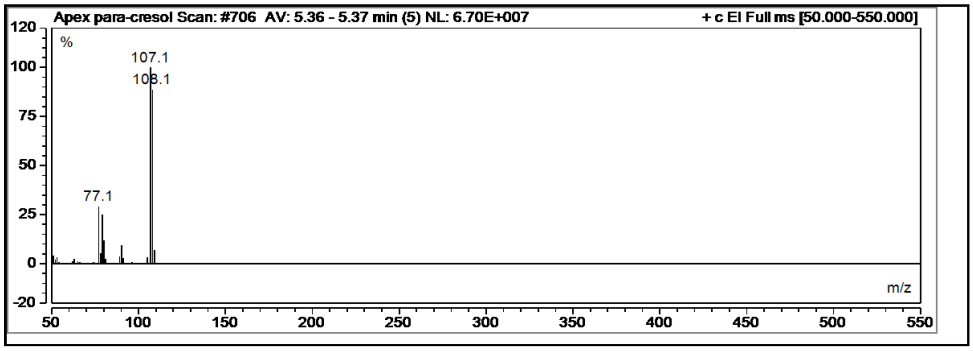

Figure 2.8. Mass spectrum of para-cresol. Base peak at m/z 107.1 on Thermo Scientific Trace 1310 Gas Chromatograph equipped with a Restek Rtx-5MS column and TSQ 9000.

2.2.2 Internal standard selection

To quantify cresols, an internal standard method was chosen to ensure accurate analyte quantification by compensating for possible variations in the sample preparation, injection volume, or instrumental response. Caffeine was selected based on the following criteria: it does not naturally occur in the bark, is stable, and can be readily ionized. However, due to the poor solubility of caffeine in methanol, water was chosen as a co-solvent to enhance its solubility.

2.2.3 Calibration and validation

The linearity of cresol isomers was assessed for a 10-fold concentration range, 20 – 200 mg/L, with the addition of 20 mg/L of caffeine. Calibration curves for cresol isomers were plotted by the ratio of peak areas of the isomer and the internal standard versus the sample concentrations (Figure 2.9). All cresols expressed linearity in the 20 – 200 mg/L range with a correlation coefficient (R^2) > 0.99. Following the calculations described by Apostol and co-workers,[31] the assessments of the limit of detection (LOD) and limit of quantification (LOQ) for each isomer were based on the Standard Deviation of the y-intercept from the regression of their respective calibration curve. The LOD values for *ortho*-, *meta*-, and *para*-cresol are 20.6 mg/L, 16.6 mg/L, and 14.2 mg/L (Table 2.1). Similarly, the LOQ values for *ortho*-, *meta*-, and *para*-cresol were determined to be 62.6 mg/L, 50.2 mg/L, and 43.0 mg/L (Table 1.1).

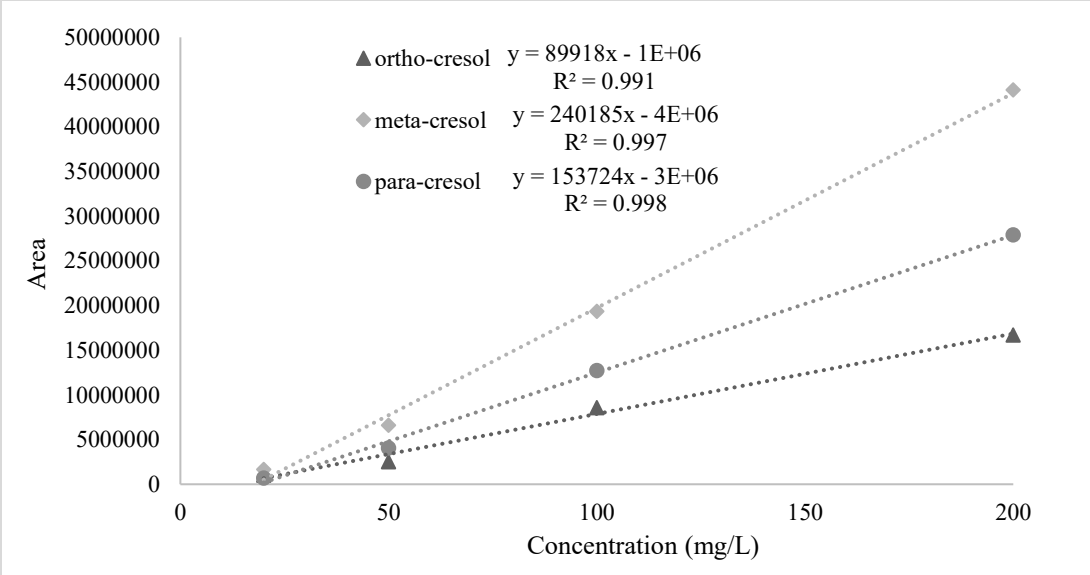

Figure 2.9. Calibration curves for cresol isomers obtained in triplicate. Peak area vs. concentration.

Table 2.1. Analytical parameters of the method for quantification of *ortho*-, *meta*- and *para*-cresol.

Analyte	**Retention time (min)**	**Linear range (mg/L)**	**Correlation coefficient (R^2)**	**LOD (mg/L)**	**LOQ (mg/L)**	**$\mu \pm \frac{t\,RSD}{\sqrt{n}}$ (mg/L)**
ortho-creso	5.204	20 – 200	0.991	20.6	62.6	324 ± 9
meta-cresol	5.345	20 – 200	0.997	16.6	50.2	871 ± 100
para-cresol	5.338	20 – 200	0.998	14.2	43.0	1,240 ± 156

LOD, limit of detection; LOQ, limit of quantification; μ, mean; t: t-value at 95% confidence level; RSD: relative standard deviation; n: number of injections (n = 6).

2.2.4 Analysis of the birch bark extract

For the characterization of a birch bark sample, an aliquot of the extract was diluted 8-fold with methanol and analyzed with the developed GC-MS method (see Figure 2.10). Cresol isomers were identified by comparing the retention time of the peaks in the calibration solutions and the sample. The base peak of each compound was chosen for quantitation (*m/z* 108.1 for *ortho*- and *meta*-cresol, *m/z* 107.1 for *para*-cresol). The sample was analyzed

in quintuplicate. The obtained GC-MS total ion chromatogram (TIC) reveals a dense array of peaks, showing the complexity of the extract (see Figure 2.11). The caffeine IS elutes at 10.576 min, however, its presence is difficult to distinguish due to the high number of overlapping signals. A closer examination of the chromatogram in the region where the cresols elute indicates that the *meta*- and *para*-isomers elute together, while the *ortho* peak is obscured by interference with adjacent compounds. Following full scan analysis by GC-MS, the quantities of *ortho*-, *meta*-, and *para*-cresols in birch bark extract were determined as 324 ± 9 mg/L, 871 ± 100 mg/L, and 1,240 ± 156 mg/L, respectively. Although quantification was performed for the cresol isomers in the sample, its accuracy is uncertain due to the close elution of *m*- and *p*-isomers and from overlapping peaks.

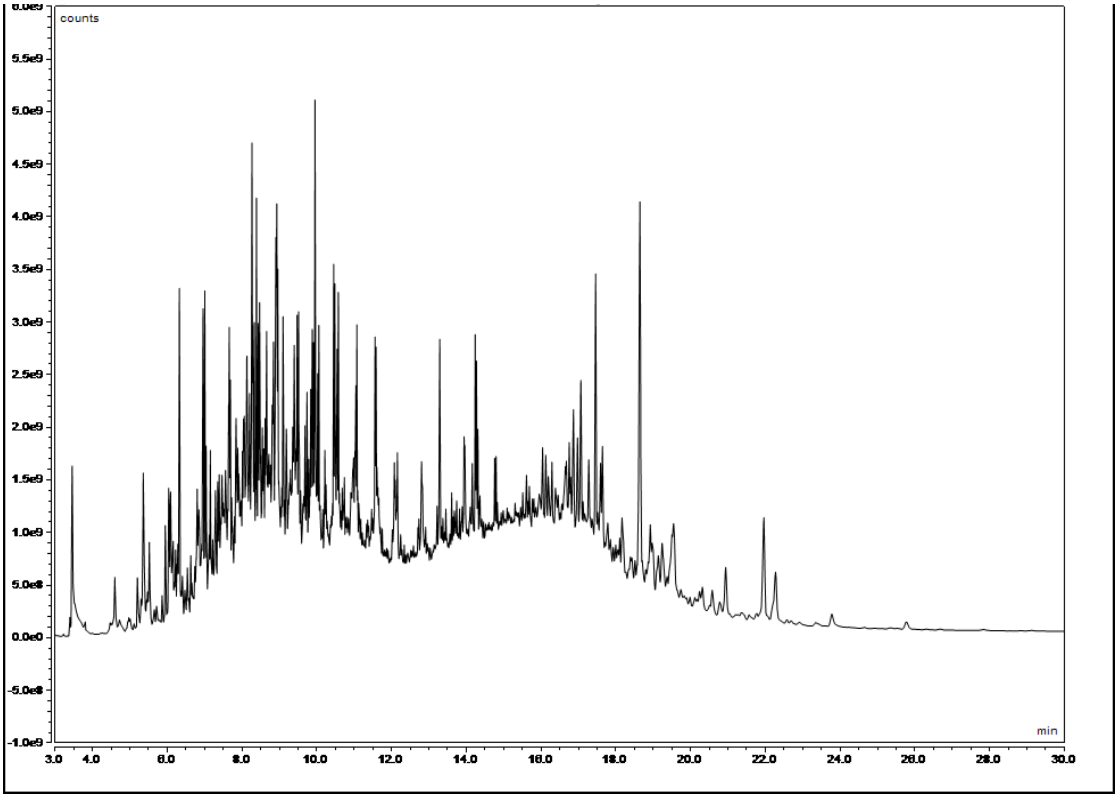

Figure 2.10. Total ion chromatogram obtained for a birch bark extract. Total run of 30 min on Thermo Scientific Trace 1310 Gas Chromatograph equipped with a Restek Rtx-5MS column and TSQ 9000.

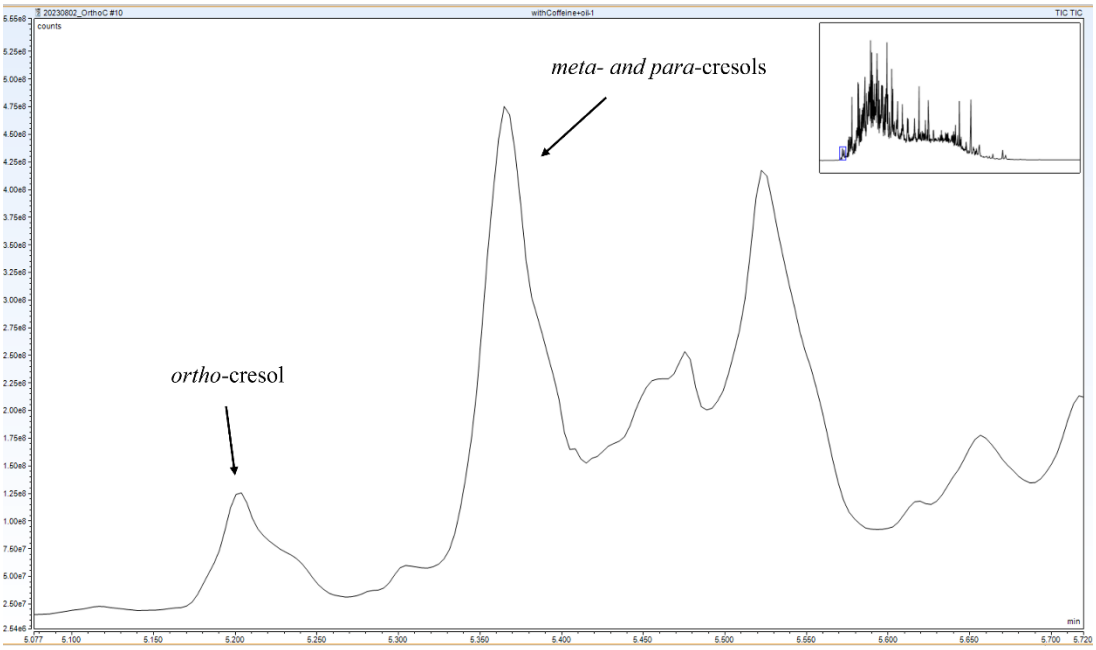

Figure 2.11. Total ion chromatogram obtained for a birch bark extract (closer examination). Ortho-cresol elutes at 5.204 min, while *m*- and *p*-isomers elute together at 3.355 min. Total run times on the Thermo Scientific Trace 1310 Gas Chromatograph-TSQ 9000 GC-MS equipped with a Restek Rtx-5MS column were 30 min.

2.3 Conclusions

A full-scan GC-MS method was developed to detect and quantify three cresol isomers in the birch bark extract with caffeine as an internal standard. The separation of *meta*- and *para*-cresol is difficult due to their similar boiling points. Despite high interference from overlapping peaks, *ortho*-, *meta*-, and *para*-cresol in birch bark extract were determined to be 324 mg/L, 871 mg/L, and 1,240 mg/L, respectively. A different approach, such as selected reaction monitoring, needs to be taken to quantify the cresol isomers efficiently.

2.4 Experimental

2.4.1 Materials

Ortho-cresol, *meta*-cresol, *para*-cresol, and caffeine were obtained from Sigma-Aldrich (MilliporeSigma Canada Ltd., ON, Canada). Methanol was purchased from Fisher Scientific (Thermo Fisher Scientific Inc., Waltham, MA, USA). All chemicals and solvents used were of analytical grade.

2.4.2 Extraction method

White paper birch bark (*Betula papyrifera* Marshall) was collected from fallen birch trees. The outer bark was separated from the inner bark, washed with water, and dried. The reactor system was built by the lab, and the procedure can be described as follows. The wired basket is filled with shredded bark and secured with wire mesh. The basket is placed in the reactor vessel, sealed with the lid, and insulated. The cooling system is activated to maintain proper flow. The reactor vessel is programmed to the optimized conditions using a proportional–integral–derivative controller, connected to a computer via the Omega datalogger. The temperature was ramped to 300 °C at 600.0 °C/min with a hold of 30.0 min, then ramped to 425 °C at 300.0 °C/min with a hold of 20.0 min. Finally, it was ramped to 500 °C at 100.0 °C/min and held for 30.0 min.

2.4.3 Sample preparation

All cresol standard solutions were prepared in methanol from a 10,000 mg/L stock with a pipette, forming concentrations of 40, 100, 200, 400, and 1,000 mg/L. Afterward, 1.0 mL

of each solution was mixed with 1.0 mL of a 40 mg/L caffeine solution, which was used as an internal standard (IS) and vortexed. A 40 mg/L solution of caffeine was prepared from a 10,000 mg/L stock in a co-solvent mixture (methanol:water (50:50)% v/v). Before analysis, 0.4357 g of birch bark extract was dissolved in 4 mL methanol, then a 1.0-mL aliquot of the prepared solution was mixed with 1.0 mL of methanol and vortexed. Calibration curves were obtained in triplicate.

2.4.4 GC-MS conditions

A Thermo Scientific TRACE 1310 gas chromatograph (Thermo Fisher Scientific Inc., Waltham, MA, USA) equipped with an EI source and a Thermo Scientific TSQ 9000 Triple Quadrupole Mass Spectrometer (Thermo Fisher Scientific Inc., Waltham, MA, USA) were used for the identification of cresols in the birch bark extract. The oven temperature was kept at 50 °C for 1.0 min, ramped to 200 °C at 10.0 °C /min with a hold of 5.0 min, then ramped again to 280 °C at 15.0 °C /min with a hold of 5.0 min. Helium with a purity of 99.9999% was used as a carrier gas with a flow rate of 5.0 mL/min. the chromatographic separation was achieved by an Rtx-5MS (30.0 m × 250.0 µm × 0.25 µm) capillary column obtained from Restek (Restek Corp., Centre County, PA, USA) and injections were performed by TriPlus RSH autosampler (Thermo Fisher Scientific Inc., Waltham, MA, USA) in a splitless mode. The overall run time was 30.0 min. The triple quadrupole MS provided at least unit resolution over the scan range *m/z* 50 – 550. The MS transfer-line and ion source temperatures were 250 °C and 230 °C, respectively.

Chapter 3. Quantitative analysis of phenolic compounds by time-dependent selected reaction monitoring-based GC-MS/MS method

3.1 Introduction

GC-MS is a preferred technique for the quantification of phenolic compounds yet its application for complex matrices remains challenging. SRM, referred to as multiple reaction monitoring (MRM) when multiple transitions are included, is an alternative approach for the accurate quantification of low-abundant targeted compounds typically employing a triple quadrupole (QqQ) instrument.[110] By selecting a specific precursor-to-product ion transition, SRM provides high selectivity, enhanced sensitivity, and reduced interference from the matrix.[111] In an SRM assay, the first quadrupole mass analyzer (Q1) is initially set to allow only a precursor ion specific to a targeted compound to pass through. The ion undergoes fragmentation by collision-induced dissociation (CID) in the collision cell (Q2). Finally, the second quadrupole mass analyzer (Q3) filters so that only a specific fragment ion maintains a stable trajectory under the optimized collision energy. The two m/z selection minimize the background signal and provide a high duty cycle.[112]

3.2 Results and discussion

The objective of this study was (a) to develop MRM methods and quantify several phenolic compounds in *Betula papyrifera* extract, and (b) to compare the quantified amounts obtained using full scan to MRM. Standard solutions, extract samples, and spiked solutions

were analyzed using the TSQ 9000 triple quadrupole GC-MS system to achieve this. The established methods were then validated by assessing linearity, intra- and inter-day precision, limit of detection (LOD) and quantification (LOQ) of targeted compounds. Finally, the methods were applied to the quantitative analysis of phenolic compounds and triterpenes in *Betula papyrifera* extract with its accuracy evaluated by recovery checks.

3.2.1 Method development for qualitative identification of targeted phenolic compounds

Initially, the detection of each compound standard was performed using the full scan acquisition mode using the instrumental conditions selected in Chapter 2. The GC temperature programming for phenolics was shortened to a 15-minute run, as mentioned in Section 2.1.1. Full scan, product ion scans, and optimization of MRM conditions were then conducted to select precursor ions, product ions, and optimized collision energies for an optimized method for each compound. Two SRM transitions for each compound were chosen; a caffeine IS (20 mg/L) was used to ensure greater accuracy (Table 3.1).

Table 3.1. SRM transitions selected for phenolic compounds.

Compound	**Retention time (min)**	**Precursor ion (*m/z*)**	**Product ion (*m/z*)**	**Collision energy (eV)**
caffeine	10.522	194.1	109.1	12
		194.1	193.1	8
ortho-cresol	5.196	108.1	79.1	14
		108.1	107.1	12
meta-cresol	5.377	107.0	51.1	24
		107.0	77.1	14
para-cresol	5.354	108.1	79.1	14
		108.1	107.1	12
2-methoxyphenol	5.525	124.1	81.0	10
		124.1	109.0	18
4-allyl-2-methoxyphenol	7.546	164.1	77.0	8
		164.1	149.1	14
4-methoxyphenol	6.491	124.1	53.1	16
		124.1	81.0	26
benzene-1,2-diol	6.341	63.1	62.1	6
		64.1	63.1	16
benzene-1,3-diol	6.757	81.1	53.1	8
		82.1	81.1	6
4-hydroxy-3-methoxybenzaldehyde	7.836	123.1	65.1	14
		123.1	108.0	8

3.2.2 Method validation

Prior to the quantitative analysis of selected compounds, the methods developed were validated by linearity, limits of detection (LODs), limits of quantification (LOQs), and precision. The data (Table 3.2) shows the linear ranges, LODs, and LOQs. The linearity of calibration curves for the targeted compounds was assessed by analyzing standard solutions at five calibration levels. Linear regression curves were plotted using the average values of n = 2 injections per calibration level. All curves showed a good linearity with correlation coefficients (R^2) ranging from 0.983 to 0.998 within the test range. The LODs and LOQs were measured with signal-to-noise ratios (S/N) of 3 and 10, respectively, and were determined based on the residuals standard deviation method. The amounts determined for each analyte varied from 0.4 – 21.8 mg/L for LOD and 1.3 – 66.2 mg/L for LOQ.

Table 3.2. Analytical parameters of the method for quantification of targeted compounds.

Compound	**Linear range (mg/L)**	**R^2**	**LOD (mg/L)**	**LOQ (mg/L)**
ortho-cresol	20 – 100	0.991	0.4	1.3
meta-cresol	20 – 100	0.998	4.6	14.0
para-cresol	20 – 100	0.983	13.6	41.1
2-methoxyphenol	20 – 100	0.996	6.3	19.1
4-allyl-2-methoxyphenol	20 – 100	0.991	7.9	23.8
4-methoxyphenol	20 – 100	0.996	21.8	66.2
benzene-1,2-diol	20 – 100	0.998	4.8	14.6
benzene-1,3-diol	20 – 100	0.996	10.2	31.0
4-hydroxy-3-methoxybenzaldehyde	20 – 100	0.992	7.4	22.5

LOD, limit of detection; LOQ, limit of quantification.

Intra- and inter-day precision of the MRM methods were evaluated based on an average of 6 injections on a single day and an average of 6 injections over two consecutive days (Table 3.3). Calibration curves exhibited acceptable precision as intra-day RSD ranged from 1.7 – 7.7%, whereas inter-day RSD ranged from 3.5 – 11.4%.

Table 3.3. Intra-day and inter-day precision for quantification of targeted compounds.

Compound	**Intra-day precision RSD (%) [a]**	**Inter-day precision RSD (%) [b]**
ortho-cresol	7.2	11.4
meta-cresol	2.2	3.6
para-cresol	7.7	9.2
2-methoxyphenol	2.8	3.5
4-allyl-2-methoxyphenol	3.9	4.7
4-methoxyphenol	2.2	3.9
benzene-1,2-diol	1.7	7.0
benzene-1,3-diol	4.4	8.7
4-hydroxy-3-methoxybenzaldehyde	3.7	8.3

RSD: relative standard deviation; a: based on an average of 6 injections on the same day; b: based on an average of 6 injections over two consecutive days.

3.2.3 Qualitative analysis of 9 compounds in *Betula papyrifera* extract

The developed GC-MS/t-SRM method was then applied to the quantification of nine compounds in *Betula papyrifera* extract. As previously mentioned, the sample extracts were prepared by 8-fold dilution with methanol. Table 3.4 presents the confidence interval for the determined amounts, based on an average of six injections for each sample, along with the standard deviation of their respective peak area. The results indicate that all

compounds were present in *Betula papyrifera* extract, with varying quantities. The highest concentration was detected for benzene-1,2-diol (5,909 ± 141 mg/L), followed by *m*-cresol (1,708 ± 14 mg/L) and *p*-cresol (1,487 ± 19 mg/L), respectively.

Table 3.4. Compounds determined in *Betula papyrifera* extract.

Compound	**Retention time (min)**	**$\mu \pm \frac{t\ RSD}{\sqrt{n}}$ (mg/L)**	**Peak area RSD (%)**
ortho-cresol	5.196	652 ± 15	1.6
meta-cresol	5.377	1,708 ± 14	0.6
para-cresol	5.354	1,487± 19	1.1
2-methoxyphenol	5.525	673 ± 31	1.1
4-allyl-2-methoxyphenol	7.546	299 ± 2	3.0
4-methoxyphenol	6.491	192 ± 4	6.0
benzene-1,2-diol	6.341	5,909 ± 141	1.3
benzene-1,3-diol	6.757	362 ± 1	1.6
4-hydroxy-3-methoxybenzaldehyde	7.836	348 ± 1	0.9

μ, mean; t: t-value at 95% confidence level; RSD: relative standard deviation; (n = 6).

3.3 Conclusions

Nine compounds were effectively quantified in birch bark extract via GC-MS/t-SRM. The determined amounts varied from 192 to 5,909 mg/L with a precision of ≤ 6%. The developed method allowed a highly selective analysis of compounds despite challenging matrix interference.

3.4 Experimental

3.4.1 Materials

O-cresol, *m*-cresol, *p*-cresol, benzene-1,2-diol, benzene-1,3-diol, 2-methoxyphenol, 4- methoxyphenol, 4-hydroxy-3-methoxybenzaldehyde, 4-allyl-2-methoxyphenol, and caffeine were obtained from Sigma-Aldrich (MilliporeSigma Canada Ltd., Ontario, Canada). Methanol was purchased from Fisher Scientific (Thermo Fisher Scientific Inc., Waltham, MA, USA). All chemicals and solvents used were of analytical grade.

3.4.2 Extraction method

The extraction method employed follows the procedure detailed in Section 2.4.2.

3.4.3 Calibration and validation

All standard solutions were prepared in methanol from a 10,000 mg/L stock with a micropipette, forming concentrations of 40, 80, 120, 160, and 200 mg/L. Afterward, 1 mL of each solution was mixed with 1.0 mL of 40 mg/L caffeine solution used as an internal standard and vortexed. A 40 mg/L caffeine solution was prepared from a 10,000 mg/L stock in methanol and sonicated. The intra- and inter-day precision was performed by consequently analyzing standards in sextuplicate. Intra-day and inter-day tests were conducted on the same day and over two consecutive days.

3.4.4 Sample preparation

Before analysis, 0.3500 g of the birch bark extract was dissolved in 2 mL methanol and sonicated for 2 h, then a 1.0 mL aliquot of the solution was mixed with 1.0 mL of 40 mg/L caffeine solution and vortexed. Calibration curves were obtained in triplicate.

3.4.5 GC-MS conditions

The instrumental conditions for the selected reaction monitoring (SRM) establishment were consistent with those described in Section 2.4.4. Data acquisition was performed using the timed-SRM approach, with further collision energy optimization, then processed by Thermo Scientific Chromeleon software. For the detailed procedure, refer to Section 2.4.4.

Chapter 4. Determination of triterpenes by UHPLC-APCI-QTOF-MS method

4.1 Introduction

LC-MS is widely used in detecting triterpenes due to its ability to analyze non-volatile and thermally unstable compounds without derivatization. Among LC-MS techniques, ESI is commonly employed for polar triterpenes, such as oleanolic or ursolic acids, while atmospheric pressure chemical ionization (APCI) and atmospheric pressure photoionization (APPI) are selected for less polar triterpenes that cannot be ionized efficiently by ESI.[113] The ionization efficiency of these atmospheric pressure sources was evaluated for 12 triterpenes, with both APCI and APPI being effective for triterpenes detection.[113] APCI primarily depends on source temperature and the corona discharge needle current. In contrast, APPI requires additional parameter adjustments, particularly source temperature and dopant selection. Despite the complexity, APPI has been demonstrated to have higher sensitivity than APCI in positive ion mode. For example, the limits of quantification (LOQ) for lupeol, betulin, betulin derivatives, and other triterpenoids in selected ion mode (SIM) ranged from 5 – 15 µg/L for APPI and 2 – 840 µg/L for APCI.[113] UHPLC-APPI-MS conditions have also been applied for triterpenes analysis using MRM and assessed for precision and accuracy.[114] The LOQ values for lupeol and betulinic acid were similar to each other at 6.6 and 6.7 µg/L, respectively. Another MRM-based UHPLC-APCI-MS method was developed for the analysis of four triterpenes (lupeol, erythrodiol, betulin, and betulinic acid).[115] The limits of quantification were in the range of 2 – 6 µg/L, with compounds containing two hydroxyl

groups demonstrating higher LOQ values. In comparison, UHPLC-ESI-MRM-MS provided an even lower LOQ for betulinic acid at 0.35 μg/L.[116]

The work reported in this chapter was directed toward development of a UHPLC- QTOF- MS method for the detection and quantification of betulin and betulinic acid.

4.2 Results and discussion

4.2.1 Method development

The first step in the method development was to select an ionization source that could provide efficient ionization and accurate quantification of the analytes. This choice is critical as it directly impacts the sensitivity, specificity, and overall analytical performance. Among the available techniques, ESI and APCI are most used for complex matrices.[117].While ESI, more suitable for polar and ionic compounds, was initially tested, it proved to be insufficient for the quantification of the targeted triterpenes due to its preferential ionization of impurities rather than betulin (Figure 4.1). APCI was therefore selected as it offered superior performance, particularly for analyzing less polar compounds like triterpenes.

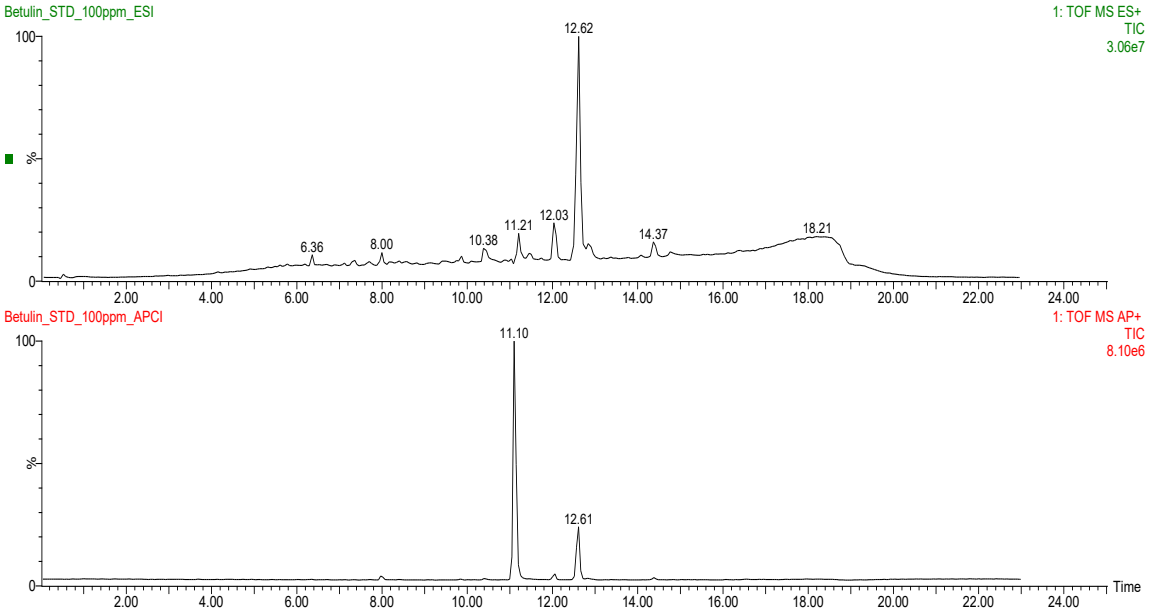

Figure 4.1. Chromatograms of 100 mg/L betulin standard using ESI and APCI.

For the chromatographic separation, a BEH (ethylene-bridged hybrid) C18 column was chosen due to its chemical stability over a wide pH range (1 – 12) and its ability to provide high-resolution separation of structurally similar compounds. The ionization polarity was evaluated to optimize sensitivity and selectivity for triterpenes detection. Both positive and negative ionization modes were tested using APCI-MS. The positive mode demonstrated better performance, given higher peak intensity and well-defined chromatographic peaks (Figure 4.2). In contrast, the negative mode exhibited lower signal intensity and lower resolution as more interferences appeared in the TIC, with prominent peaks attributed to impurities rather than the standard compound.

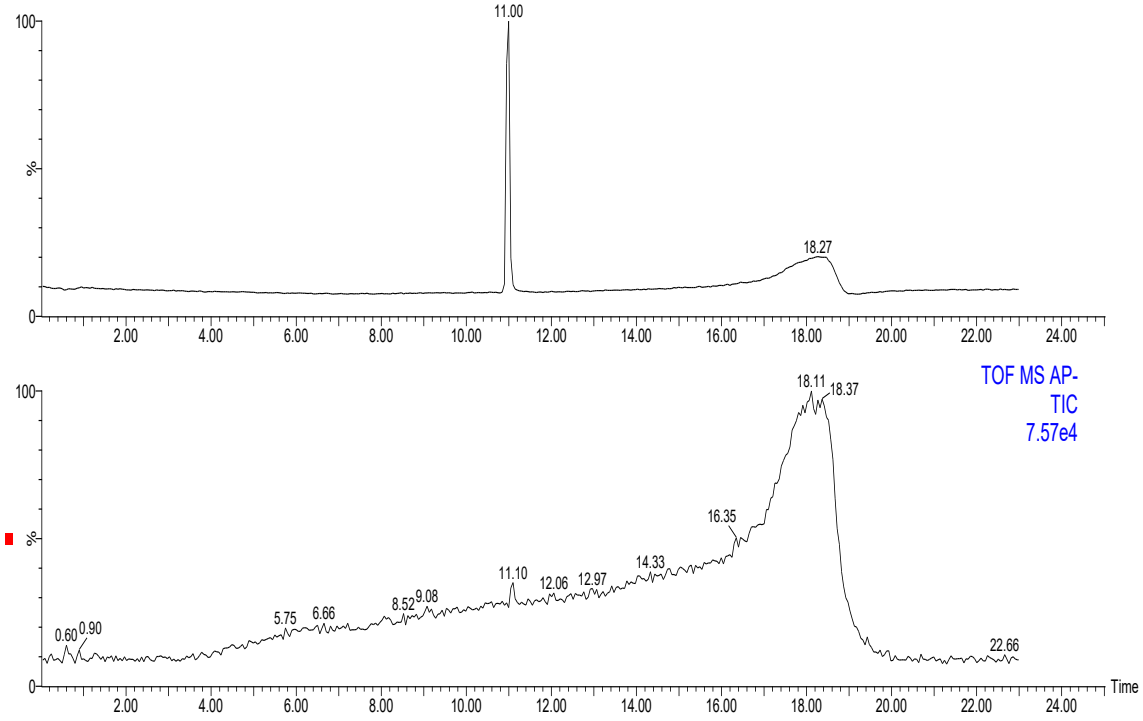

Figure 4.2. Chromatograms of 100 mg/L betulin standard using positive and negative ion mode APCI.

A gradient elution method was chosen to allow better resolution and improve the sensitivity of the analysis. The mobile phase composition underwent optimization. Initially, acetonitrile was used as the organic solvent, but it was replaced with methanol as the latter provided better solubility (for the sample) and enhanced ionization for the triterpenes under APCI conditions. The compatibility of methanol with APCI, along with improved chromatographic peak shapes and higher signal intensities, make it the preferred choice. The source conditions were optimized for both betulin and betulinic acid by testing the parameters (Table 4.1).

Table 4.1.Tested parameters and optimized conditions for analysis of triterpenes.

Tested parameter	Tested	Optimized for betulin	Optimized for betulinic acid
Flow rate (mL/min)	0.2; 0.3; 0.4	0.3	0.3
Corona current	2.0; 3.0; 4.0	4.0	4.0
Probe temperature (°C)	500; 550	550	500
Source temperature (°C)	120; 150	120	150
Desolvation gas flow (L/h)	800; 1000	800	1000

4.2.2 Qualitative analysis of betulin

The fragmentation of pentacyclic triterpenes involves a retro Diels-Alder (rDA) cleavage in the C-ring, breaking the C(8)–C(14) and C(9)–C(11) bonds to generate two fragments: the ABC* and the C*DE moieties, where * indicates the ring undergoing fragmentation [118,119]. Betulin, which elutes at 10.95 min in the TIC, its deprotonated molecular ion $[M- H]^+$ appears at *m/z* 443 (Figure 4.3). The molecular ion $[M]^+$ underwent the neutral loss of a water molecule, forming the base peak at *m/z* 425 $[M-H_2O]^+$. The $[M-H_2O]^+$ ion may lose additional water molecule, producing a peak at *m/z* 407, or undergo RDA fragmentation, forming a C*DE fragment at *m/z* 235. Alternatively, the RDA process might occur to the molecular ion $[M]^+$, yielding an ABC* fragment at *m/z* 191.

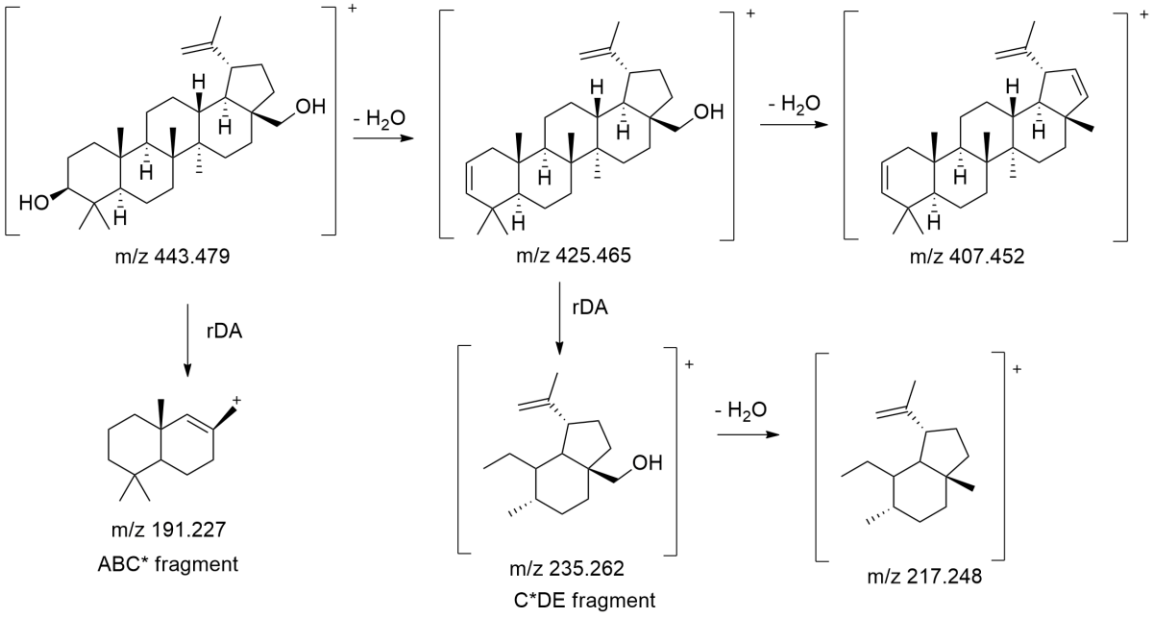

Figure 4.3. Proposed main fragments of betulin after retro Diels-Alder cleavage under APCI.

4.2.3 Method validation

To ensure the reliability of the UHPLC-APCI-QTOF method for the quantification of triterpenes in the sample, analytical parameters were evaluated, including linear range, correlation coefficient, limit of detection (LOD), and limit of quantification (LOQ). The results are summarized in Table 4.2.

Table 4.2. Analytical parameters of triterpenes analysis.

Compound	**Retention time**	**Linear range (mg/L)**	**Correlation coefficient (R^2)**	**LOD (mg/L)**	**LOQ (mg/L)**
Betulin	11.15	20 – 100	0.992	60	183
Betulinic acid	11.85	20 – 100	0.995	7.9	23.9

LOD, limit of detection; LOQ, limit of quantification.

Under optimized chromatographic conditions, betulin and betulinic acid were eluted at 11.15 min and 11.85 min, respectively. Linearity was assessed at five concentration levels ranging from 20 – 100 mg/L for both compounds, resulting in $R^2 > 0.99$, suggesting a strong positive correlation. The method demonstrated varying sensitivity levels for targeted compounds. For betulin, LOD was determined to be 60.4 mg/L, while LOQ was 183.1 mg/L. In contrast, betulinic acid demonstrated higher sensitivity at 7.9 mg/L and 23.9 mg/L levels for LOD and LOQ, respectively.

4.2.4 Quantitative analysis of triterpenes

The validated UHPLC-APCI-MS method was then applied to the quantification of two triterpenes in the *Betula papyrifera* extract. The birch bark sample was diluted 8-fold in methanol and analyzed. The results of the quantitative analysis are summarized in Table 4.3, presenting the confidence interval for the determined amounts, based on an average of six injections for each sample and the relative standard deviations (RSD) of the respective peak areas for each compound. Betulin and betulinic acid were determined to be 2,411 ± 45 mg/L and 199 ± 8 ppm, respectively, with an acceptable precision of < 5%.

Table 4.3. Triterpenes determined in *Betula papyrifera* extract.

Compound	**Retention time (min)**	**$\mu \pm \frac{t\ RSD}{\sqrt{n}}$ (mg/L)**	**Peak area RSD (%)**
Betulin	11.15	2,411 ± 45	3.2
Betulinic acid	11.85	199 ± 8	4.8

μ, mean; t: t-value at 95% confidence level; RSD: relative standard deviation; n: number of injections (n = 6).

4.3 Conclusions

A UHPLC-MS method was developed for the detection and quantification of several triterpenes in *Betula papyrifera* extract. APCI was confirmed to provide superior performance to ESI for low polarity compounds such as triterpenes. Betulin and betulinic acid in the bio-oil extracts were quantified and found to be 2,411 ± 45 ppm and 199 ± 8 ppm, respectively, with an acceptable precision of < 5%. This indicates that the method developed is reliable for the identification and quantification of other low-volatility compounds in complex matrices such as the *Betula papyrifera* extract.

4.4 Experimental

4.4.1 Materials

Betulin, betulinic acid, and caffeine were obtained from Sigma-Aldrich (MilliporeSigma Canada Ltd., Ontario, Canada). Methanol, acetone, and acetonitrile were purchased from Fisher Scientific (Thermo Fisher Scientific Inc., Waltham, MA, USA). All chemicals and solvents used were of analytical grade.

4.4.2 Extraction method

The extraction method employed follows the procedure detailed in Section 2.4.2. For the detailed method, refer to that section.

4.4.3 Calibration

A 1,000 mg/L stock solution of betulin was prepared in a binary solvent mixture using a micropipette (acetonitrile:acetone (50:50 v/v). Standard solutions of betulin were prepared in methanol from 1,000 mg/L stock, forming concentrations of 40, 80, 120, 160, and 200 mg/L. Afterward, 1.0 mL of each solution was mixed with 1.0 mL of 40 mg/L caffeine solution, which was used as an internal standard and vortexed. A 40 mg/L solution of caffeine was prepared from 10,000 mg/L stock in a binary solvent mixture (methanol:water (50:50 v/v)).

4.4.4 Sample preparation

To prepare a birch bark sample, 0.3 g of extract was dissolved in 4 mL methanol, then a 1 mL aliquot of the solution was mixed with 1 mL of methanol and vortexed. Calibration curves were obtained in triplicate.

4.4.5 UHPLC-MS conditions

UHPLC-MS was performed with an Acquity UPLC System (Waters Corp., MA, USA) with a Waters Xevo QTOF MS (Waters Corp., MA, USA) and atmospheric pressure chemical ionization as an ion source. Optimized instrument parameters were as follows: corona current at 4.0 μA; probe temperature at 550 °C for betulin and 500 °C for betulinic acid; source temperature at 120 °C for betulin and 150 °C for betulinic acid; sampling cone at 35.0 V; extraction cone at 4.0 V; cone gas flow at 50.0 L/h; desolvation gas flow at 800 L/h for betulin and 1000 L/h for betulinic acid. UHPLC separation was carried out with an Acquity UPLC BEH C18 Column (1.7 μm × 2.1 mm × 50 mm) operating at 40.0 °C

in a gradient mode. The mobile phase was A: water with 0.1% formic acid (v/v); B: acetonitrile with 0.1% formic acid (v/v). The gradient program was: Initial at B: 5%; 2 min at B: 30%; 3 min at B: 50%; 4 min at B: 70%; 8 min at B: 80%; 15 min at B: 90%; 16 min at B: 95%; 20 min at B: 95%; 25 min at B: 95%. The injection volume was 10 µL, and the flow rate was at 0.3 mL/min.

Chapter 5. Conclusions and future Work

This chapter reports the conclusions about the thesis work as well as some preliminary results from studies begun to differentiate the chemical composition of birch bark extracts obtained from traditional methods versus a controllable laboratory reactor. The results from these analyses are semi-qualitative; further analysis is needed to confirm the trends established.

5.1 Conclusions

In Chapter 2, a full-scan GC-MS method was reported to detect and quantify three cresol isomers in the birch bark extract using caffeine as an internal standard. Despite high interference from overlapping peaks in birch bark extract, *ortho*-, *meta*-, and *para*-cresol were determined to be 324 mg/L, 871 mg/L, and 1,240 mg/L, respectively.

In Chapter 3, a different approach, such as selected reaction monitoring, was taken for the quantification of nine compounds, including cresols in birch bark extract. The determined amounts ranged from 192 to 5,909 mg/L with a precision of ≤ 6%.

In Chapter 4, a UHPLC-MS method was developed for the detection and quantification of several triterpenes in *Betula papyrifera* extract. APCI was confirmed to provide superior performance for low polar compounds such as triterpenes compared to ESI. Betulin and betulinic acid were quantified at concentrations of 2,411 ± 45 ppm and 199 ± 8 ppm, respectively, both demonstrating an acceptable precision of < 5%.

5.2 Preliminary results for analysis of bio-oil extracts from the traditional preparation method

An extract was obtained by a traditional Mi'kmaq method with a yield of 5%. The GC- MS chromatogram of the *Betula papyrifera* extract is presented in Figure 5.1. According to the National Institute of Standards and Technology (NIST) library guidelines, values of Reverse Search Index (RSI) over 800 are indicative of a good match. Thus, the present study reports the compounds with RSI values of 800 or higher. The GC-MS analysis revealed the presence of 329 peaks, with 77 matched with the NIST database. Polycyclic derivatives at 13.20% were the predominant class of compounds (Figure 5.2), followed by triterpenes, benzene, and phenol derivatives at 8.07%, 3.91%, and 3.38%, respectively. The other classes were present at less than 1%.

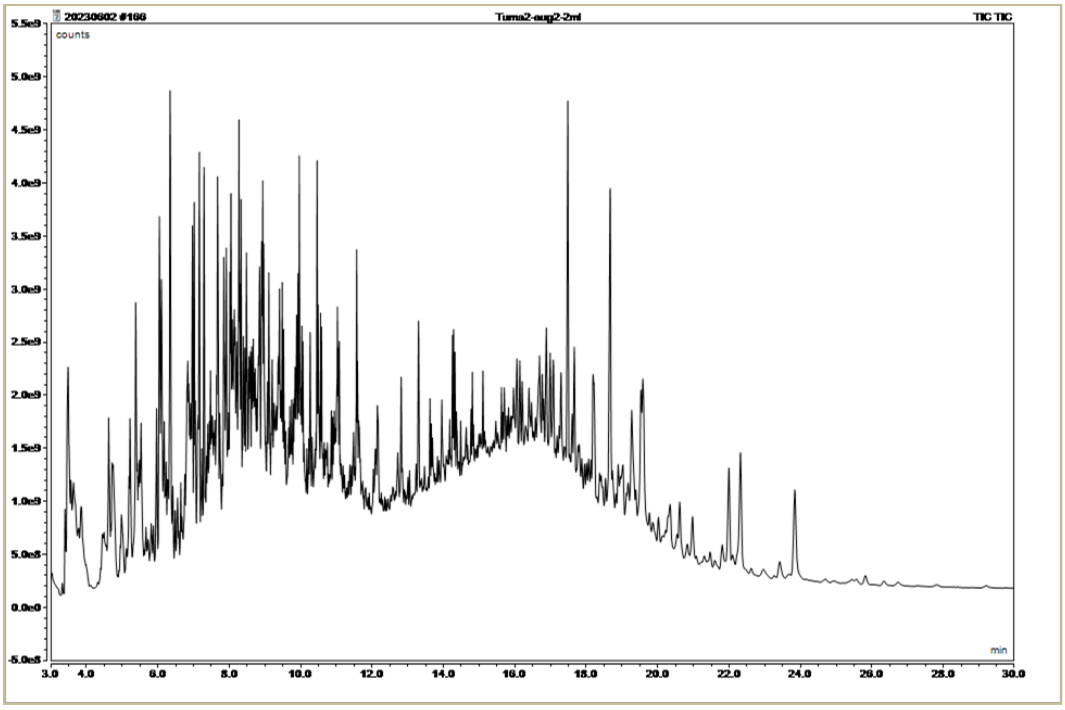

Figure 5.1. TIC of birch bark extract obtained by traditional method.

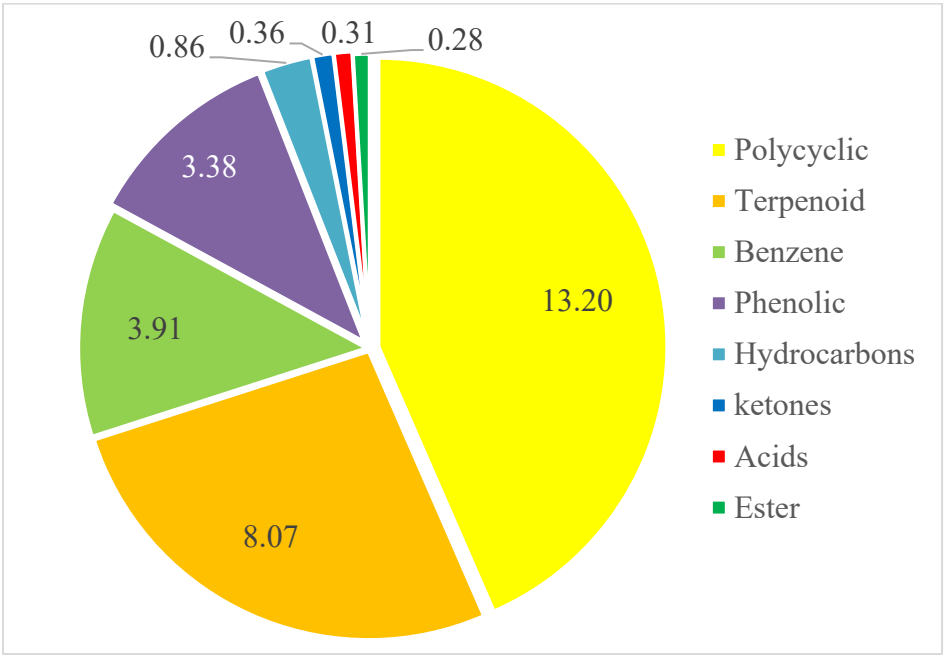

Figure 5.2. Tentative composition of birch bark extract obtained by traditional method. Identified ~31% of the total peak area.

5.3 Reactor system extract

An extract was obtained by a reactor system with a yield of 61%. The GC-MS chromatogram of the *Betula papyrifera* extract is presented in Figure 5.3. The GC-MS analysis revealed the presence of 255 peaks, with 76 matched with the NIST database. Phenolic derivatives at 16.26% were the predominant class of compounds (Figure 5.4), followed by polycyclic, triterpenes derivatives, and hydrocarbons at 9.39%, 7.20%, and 2.31%, respectively. The other classes were present at less than 2%.

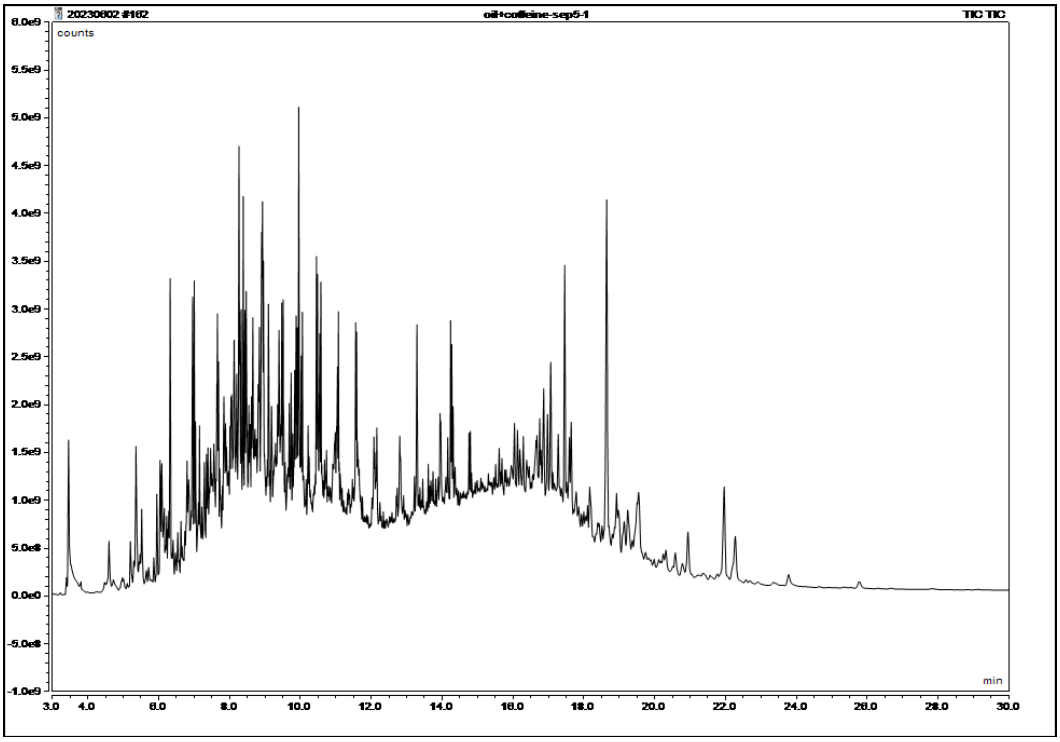

Figure 5.3. Total ion chromatogram (TIC) of birch bark extract obtained by the reactor system.

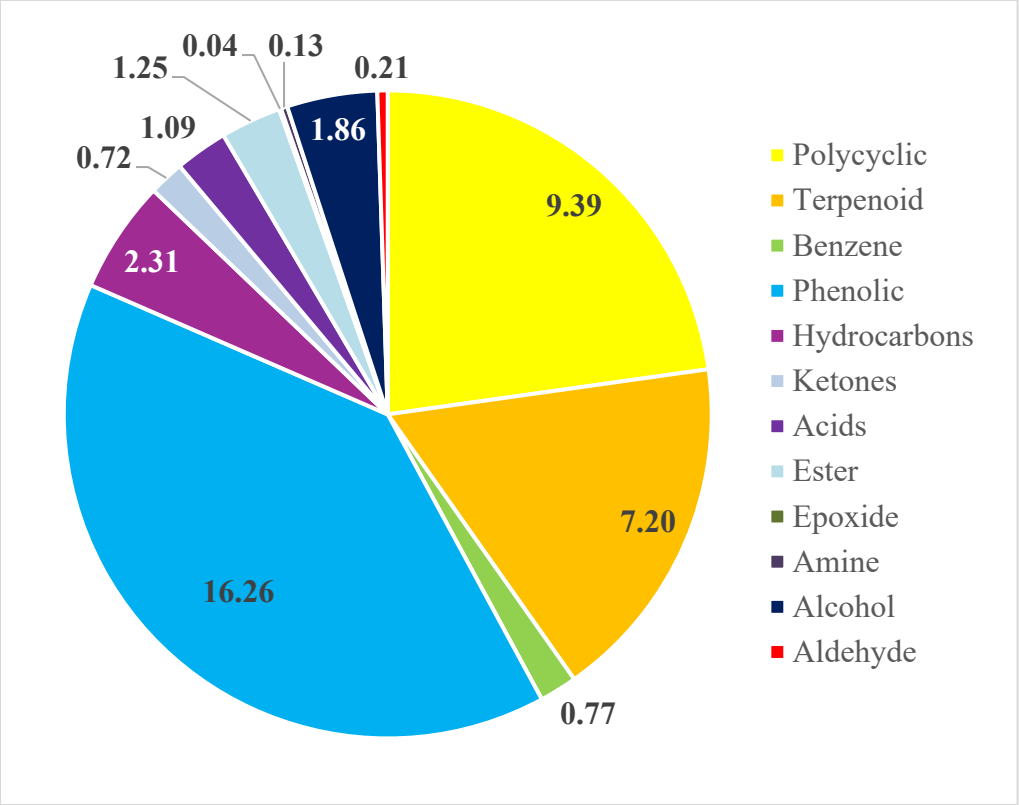

Figure 5.4. Tentative composition of birch bark extract obtained by the reactor system. Identified ~41% of the total peak area.

5.4 Experimental

White birch bark (*Betula papyrifera* Marshall) was collected from fallen birch trees, then the outer bark was separated from the inner bark, washed, and dried. The bark was placed inside a 3.5 L metal container with 4 to 8 holes at the bottom, while a 250 mL container was used as a receptacle can (Figure 1.4). It was placed flush with the ground level in a hole dug with a bark-filled container positioned atop it. After stabilizing with dirt or sand, a fire is built around the container and left to burn for 2 to 3 hours. Once cooled, the bark extract is collected from the receptacle, typically 50 to 100 mL with a 25 to 50 mL water

layer. Afterward, it is stored in the fridge until further usage. For the detailed extraction method conducted by a reactor system, refer to Section 2.4.2. For the detailed sample preparation, refer to Section 3.4.4. For the detailed GC-MS procedure, refer to Section 2.4.4.

5.5 Future work

Although some conclusions can be drawn from these results, further analysis is necessary for understanding the chemical composition of the birch bark extract. The next steps may involve targeted analysis of the compounds identified in the tentative composition (Figure 5.4), fractionation of the extract, and investigation of the influence of bark constituents (lignin, cellulose, and hemicellulose) on the overall composition of the extract.

References

(1) Harvey, A. Natural Products in Drug Discovery. *Drug Discov. Today* **2008**, *13* (19–20), 894–901. https://doi.org/10.1016/j.drudis.2008.07.004.

(2) Yuan, H.; Ma, Q.; Ye, L.; Piao, G. The Traditional Medicine and Modern Medicine from Natural Products. *Molecules* **2016**, *21* (5), 559. https://doi.org/10.3390/molecules21050559.

(3) Cragg, G. M.; Newman, D. J. Natural Products as Sources of Anticancer Agents: Current Approaches and Perspectives. In *Natural Products as Source of Molecules with Therapeutic Potential*; Cechinel Filho, V., Ed.; Springer International Publishing: Cham, 2018; pp 309–331. https://doi.org/10.1007/978-3-030-00545-0_8.

(4) Wangkheirakpam, S. Traditional and Folk Medicine as a Target for Drug Discovery. In *Natural Products and Drug Discovery*; Elsevier, 2018; pp 29–56. https://doi.org/10.1016/B978-0-08-102081-4.00002-2.

(5) Wang, J.; Xu, C.; Wong, Y. K.; Li, Y.; Liao, F.; Jiang, T.; Tu, Y. Artemisinin, the Magic Drug Discovered from Traditional Chinese Medicine. *Engineering* **2019**, *5* (1), 32–39. https://doi.org/10.1016/j.eng.2018.11.011.

(6) Cragg, G. M.; Newman, D. J.; Snader, K. M. Natural Products in Drug Discovery and Development. *J. Nat. Prod.* **1997**, *60* (1), 52–60. https://doi.org/10.1021/np9604893.

(7) Newman, D. J.; Cragg, G. M.; Snader, K. M. Natural Products as Sources of New Drugs over the Period 1981−2002. *J. Nat. Prod.* **2003**, *66* (7), 1022–1037. https://doi.org/10.1021/np030096l.

(8) Newman, D. J.; Cragg, G. M. Natural Products as Sources of New Drugs from 1981 to 2014. *J. Nat. Prod.* **2016**, *79* (3), 629–661. https://doi.org/10.1021/acs.jnatprod.5b01055.

(9) Newman, D. J.; Cragg, G. M. Natural Products as Sources of New Drugs over the Nearly Four Decades from 01/1981 to 09/2019. *J. Nat. Prod.* **2020**, *83* (3), 770–803. https://doi.org/10.1021/acs.jnatprod.9b01285.

(10) Borman, S. Combinatorial Chemistry. *Chem. Eng. News* **2002**, *80* (45), 43–43.

(11) Koehn, F. E.; Carter, G. T. The Evolving Role of Natural Products in Drug Discovery. *Nat. Rev. Drug Discov.* **2005**, *4* (3), 206–220.

(12) Lee, J.; Hyun, C.-G. Natural Products for Cosmetic Applications. *Molecules* **2023**, *28* (2), 534. https://doi.org/10.3390/molecules28020534.

(13) Cuanalo-Contreras, K.; Moreno-Gonzalez, I. Natural Products as Modulators of the Proteostasis Machinery: Implications in Neurodegenerative Diseases. *Int. J. Mol. Sci.* **2019**, *20* (19), 4666. https://doi.org/10.3390/ijms20194666.

(14) Gründemann, C.; Gruber, C. W.; Hertrampf, A.; Zehl, M.; Kopp, B.; Huber, R. An Aqueous Birch Leaf Extract of Betula Pendula Inhibits the Growth and Cell Division of Inflammatory Lymphocytes. *J. Ethnopharmacol.* **2011**, *136* (3), 444–451. https://doi.org/10.1016/j.jep.2011.05.018.

(15) Šarić-Kundalić, B.; Dobeš, C.; Klatte-Asselmeyer, V.; Saukel, J. Ethnobotanical Study on Medicinal Use of Wild and Cultivated Plants in Middle, South and West Bosnia and Herzegovina. *J. Ethnopharmacol.* **2010**, *131* (1), 33–55. https://doi.org/10.1016/j.jep.2010.05.061.

(16) Pal, M.; Mishra, T.; Kumar, A.; Baleshwar; Upreti, D. K.; Rana, T. S. Chemical Constituents and Antimicrobial Potential of Essential Oil from *Betula Utilis* Growing in High Altitude of Himalaya (India). *J. Essent. Oil Bear. Plants* **2015**, *18* (5), 1078–1082. https://doi.org/10.1080/0972060X.2015.1036569.

(17) Lans, C. Possible Similarities between the Folk Medicine Historically Used by First Nations and American Indians in North America and the Ethnoveterinary Knowledge Currently Used in British Columbia, Canada. *J. Ethnopharmacol.* **2016**, *192*, 53–66. https://doi.org/10.1016/j.jep.2016.07.004.

(18) Rastogi, S.; Pandey, M. M.; Kumar Singh Rawat, A. Medicinal Plants of the Genus Betula—Traditional Uses and a Phytochemical–Pharmacological Review. *J. Ethnopharmacol.* **2015**, *159*, 62–83. https://doi.org/10.1016/j.jep.2014.11.010.

(19) Drenkhan, R.; Kaldmäe, H.; Silm, M.; Adamson, K.; Bleive, U.; Aluvee, A.; Erik, M.; Raal, A. Comparative Analyses of Bioactive Compounds in Inonotus Obliquus Conks Growing on Alnus and Betula. *Biomolecules* **2022**, *12* (9), 1178. https://doi.org/10.3390/biom12091178.

(20) Malfa, G. A.; Tomasello, B.; Acquaviva, R.; Genovese, C.; La Mantia, A.; Cammarata, F. P.; Ragusa, M.; Renis, M.; Di Giacomo, C. Betula Etnensis Raf. (Betulaceae) Extract Induced HO-1 Expression and Ferroptosis Cell Death in Human Colon Cancer Cells. *Int. J. Mol. Sci.* **2019**, *20* (11), 2723. https://doi.org/10.3390/ijms20112723.

(21) Ghimire, B. K.; Tamang, J. P.; Yu, C. Y.; Jung, S. J.; Chung, I. M. Antioxidant, Antimicrobial Activity and Inhibition of α-Glucosidase Activity by *Betula Alnoides* Buch. Bark Extract and Their Relationship with Polyphenolic Compounds

Concentration. *Immunopharmacol. Immunotoxicol.* **2012**, *34* (5), 824–831. https://doi.org/10.3109/08923973.2012.661739.

(22) O'Connell, M. M.; Bentley, M. D.; Campbell, C. S.; Cole, B. J. W. Betulin and Lupeol in Bark from Four White-Barked Birches. *Phytochemistry* **1988**, *27* (7), 2175–2176. https://doi.org/10.1016/0031-9422(88)80120-1.

(23) Dehelean, C. A.; Şoica, C.; Ledeţi, I.; Aluaş, M.; Zupko, I.; Găluşcan, A.; Cinta-Pinzaru, S.; Munteanu, M. Study of the Betulin Enriched Birch Bark Extracts Effects on Human Carcinoma Cells and Ear Inflammation. *Chem. Cent. J.* **2012**, *6* (1), 137. https://doi.org/10.1186/1752-153X-6-137.

(24) Diouf, P. N.; Stevanovic, T.; Boutin, Y. The Effect of Extraction Process on Polyphenol Content, Triterpene Composition and Bioactivity of Yellow Birch (Betula Alleghaniensis Britton) Extracts. *Ind. Crops Prod.* **2009**, *30* (2), 297–303. https://doi.org/10.1016/j.indcrop.2009.05.008.

(25) Szoka, L.; Nazaruk, J.; Stocki, M.; Isidorov, V. Santin and Cirsimaritin from *Betula Pubescens* and *Betula Pendula* Buds Induce Apoptosis in Human Digestive System Cancer Cells. *J. Cell. Mol. Med.* **2021**, *25* (24), 11085–11096. https://doi.org/10.1111/jcmm.17031.

(26) Suresh, S.; Srivastava, V. C.; Mishra, I. M. Adsorption of Catechol, Resorcinol, Hydroquinone, and Their Derivatives: A Review. *Int. J. Energy Environ. Eng.* **2012**, *3* (1), 32. https://doi.org/10.1186/2251-6832-3-32.

(27) Heim, K. E.; Tagliaferro, A. R.; Bobilya, D. J. Flavonoid Antioxidants: Chemistry, Metabolism and Structure-Activity Relationships. *J. Nutr. Biochem.* **2002**, *13* (10), 572–584. https://doi.org/10.1016/S0955-2863(02)00208-5.

(28) Pedrielli, P.; Skibsted, L. H. Antioxidant Synergy and Regeneration Effect of Quercetin, (−)-Epicatechin, and (+)-Catechin on α-Tocopherol in Homogeneous Solutions of Peroxidating Methyl Linoleate. *J. Agric. Food Chem.* **2002**, *50* (24), 7138–7144. https://doi.org/10.1021/jf020437l.

(29) Pietta, P.-G. Flavonoids as Antioxidants. *J. Nat. Prod.* **2000**, *63* (7), 1035–1042. https://doi.org/10.1021/np9904509.

(30) Jiménez-González, M. A.; Álvarez, A. M.; Carral, P.; González-Vila, F. J.; Almendros, G. The Diversity of Methoxyphenols Released by Pyrolysis-Gas Chromatography as Predictor of Soil Carbon Storage. *J. Chromatogr. A* **2017**, *1508*, 130–137. https://doi.org/10.1016/j.chroma.2017.05.068.

(31) Mentasti, E.; Pelizzetti, E.; Baiocchi, C. Interactions of Fe(III) with Adrenaline, l-Dopa and Other Catechol Derivatives. *J. Inorg. Nucl. Chem.* **1976**, *38* (11), 2017–2021. https://doi.org/10.1016/0022-1902(76)80460-5.

(32) George C, A.; Chhabra, N. Resorcinol in Dermatology. *Indian J. Postgrad. Dermatol.* **2024**, *2*, 20–23. https://doi.org/10.25259/IJPGD_108_2023.

(33) Wang, S.; Luo, Z. *Pyrolysis of Biomass*; De Gruyter, 2016. https://doi.org/10.1515/9783110369632.

(34) Pettersen, R. C. The Chemical Composition of Wood. *Chem. Solid Wood* **1984**, *207*, 57–126.

(35) Brandt, A.; Gräsvik, J.; Hallett, J. P.; Welton, T. Deconstruction of Lignocellulosic Biomass with Ionic Liquids. *Green Chem.* **2013**, *15* (3), 550. https://doi.org/10.1039/c2gc36364j.

(36) Wang, S.; Dai, G.; Yang, H.; Luo, Z. Lignocellulosic Biomass Pyrolysis Mechanism: A State-of-the-Art Review. *Prog. Energy Combust. Sci.* **2017**, *62*, 33–86. https://doi.org/10.1016/j.pecs.2017.05.004.

(37) Vorwerk, S.; Somerville, S.; Somerville, C. The Role of Plant Cell Wall Polysaccharide Composition in Disease Resistance. *Trends Plant Sci.* **2004**, *9* (4), 203–209. https://doi.org/10.1016/j.tplants.2004.02.005.

(38) Chen, S.; Wang, Y.; Yu, L.; Zheng, T.; Wang, S.; Yue, Z.; Jiang, J.; Kumari, S.; Zheng, C.; Tang, H.; Li, J.; Li, Y.; Chen, J.; Zhang, W.; Kuang, H.; Robertson, J. S.; Zhao, P. X.; Li, H.; Shu, S.; Yordanov, Y. S.; Huang, H.; Goodstein, D. M.; Gai, Y.; Qi, Q.; Min, J.; Xu, C.; Wang, S.; Qu, G.-Z.; Paterson, A. H.; Sankoff, D.; Wei, H.; Liu, G.; Yang, C. Genome Sequence and Evolution of *Betula Platyphylla*. *Hortic. Res.* **2021**, *8*, 37. https://doi.org/10.1038/s41438-021-00481-7.

(39) Fukushima, R. S.; Hatfield, R. D. Comparison of the Acetyl Bromide Spectrophotometric Method with Other Analytical Lignin Methods for Determining Lignin Concentration in Forage Samples. *J. Agric. Food Chem.* **2004**, *52* (12), 3713–3720. https://doi.org/10.1021/jf035497l.

(40) Mohan, D.; Pittman, C. U.; Steele, P. H. Pyrolysis of Wood/Biomass for Bio-Oil: A Critical Review. *Energy Fuels* **2006**, *20* (3), 848–889. https://doi.org/10.1021/ef0502397.

(41) Sohi, S. P.; Krull, E.; Lopez-Capel, E.; Bol, R. A Review of Biochar and Its Use and Function in Soil. In *Advances in Agronomy*; Elsevier, 2010; Vol. 105, pp 47–82. https://doi.org/10.1016/S0065-2113(10)05002-9.

(42) Li, L.; Rowbotham, J. S.; Christopher Greenwell, H.; Dyer, P. W. An Introduction to Pyrolysis and Catalytic Pyrolysis: Versatile Techniques for Biomass Conversion. In *New and Future Developments in Catalysis*; Elsevier, 2013; pp 173–208. https://doi.org/10.1016/B978-0-444-53878-9.00009-6.

(43) Tian, H.; Hu, Q.; Wang, J.; Chen, D.; Yang, Y.; Bridgwater, A. V. Kinetic Study on the CO2 Gasification of Biochar Derived from Miscanthus at Different Processing Conditions. *Energy* **2021**, *217*, 119341. https://doi.org/10.1016/j.energy.2020.119341.

(44) Mamvura, T. A.; Pahla, G.; Muzenda, E. Torrefaction of Waste Biomass for Application in Energy Production in South Africa. *South Afr. J. Chem. Eng.* **2018**, *25*, 1–12. https://doi.org/10.1016/j.sajce.2017.11.003.

(45) *Pyrolysis Oils from Biomass: Producing, Analyzing, and Upgrading*; Soltes, E. J., Milne, T. A., Eds.; ACS Symposium Series; American Chemical Society: Washington, DC, 1988; Vol. 376. https://doi.org/10.1021/bk-1988-0376.

(46) Kan, T.; Strezov, V.; Evans, T. J. Lignocellulosic Biomass Pyrolysis: A Review of Product Properties and Effects of Pyrolysis Parameters. *Renew. Sustain. Energy Rev.* **2016**, *57*, 1126–1140.

(47) Greco, G.; Di Stasi, C.; Rego, F.; González, B.; Manyà, J. J. Effects of Slow-Pyrolysis Conditions on the Products Yields and Properties and on Exergy Efficiency: A Comprehensive Assessment for Wheat Straw. *Appl. Energy* **2020**, *279*, 115842. https://doi.org/10.1016/j.apenergy.2020.115842.

(48) Amutio, M.; Lopez, G.; Aguado, R.; Bilbao, J.; Olazar, M. Biomass Oxidative Flash Pyrolysis: Autothermal Operation, Yields and Product Properties. *Energy Fuels* **2012**, *26* (2), 1353–1362. https://doi.org/10.1021/ef201662x.

(49) Bridgwater, A. V.; Meier, D.; Radlein, D. An Overview of Fast Pyrolysis of Biomass. *Org. Geochem.* **1999**, *30* (12), 1479–1493. https://doi.org/10.1016/S0146-6380(99)00120-5.

(50) Ronsse, F.; Van Hecke, S.; Dickinson, D.; Prins, W. Production and Characterization of Slow Pyrolysis Biochar: Influence of Feedstock Type and Pyrolysis Conditions. *GCB Bioenergy* **2013**, *5* (2), 104–115. https://doi.org/10.1111/gcbb.12018.

(51) Williams, P. T.; Besler, S. The Influence of Temperature and Heating Rate on the Slow Pyrolysis of Biomass. *Renew. Energy* **1996**, *7* (3), 233–250. https://doi.org/10.1016/0960-1481(96)00006-7.

(52) Ighalo, J. O.; Iwuchukwu, F. U.; Eyankware, O. E.; Iwuozor, K. O.; Olotu, K.; Bright, O. C.; Igwegbe, C. A. Flash Pyrolysis of Biomass: A Review of Recent Advances. *Clean Technol. Environ. Policy* **2022**, *24* (8), 2349–2363. https://doi.org/10.1007/s10098-022-02339-5.

(53) Raja, S. A.; Kennedy, Z. R.; Pillai, B. C.; Lee, C. L. R. Flash Pyrolysis of Jatropha Oil Cake in Electrically Heated Fluidized Bed Reactor. *Energy* **2010**, *35* (7), 2819–2823. https://doi.org/10.1016/j.energy.2010.03.011.

(54) Thengane, S. K.; Kung, K. S.; Gomez-Barea, A.; Ghoniem, A. F. Advances in Biomass Torrefaction: Parameters, Models, Reactors, Applications, Deployment, and Market. *Prog. Energy Combust. Sci.* **2022**, *93*, 101040. https://doi.org/10.1016/j.pecs.2022.101040.

(55) Yaacob, N.; Rahman, N. A.; Matali, S.; Idris, S. S.; Alias, A. B. An Overview of Oil Palm Biomass Torrefaction: Effects of Temperature and Residence Time. *IOP Conf. Ser. Earth Environ. Sci.* **2016**, *36*, 012038. https://doi.org/10.1088/1755-1315/36/1/012038.

(56) Pakdel, H.; Roy, C.; Amen-Chen, C.; Roy, C. Phenolic Compounds from Vacuum Pyrolysis of Wood Wastes. *Can. J. Chem. Eng.* **1997**, *75* (1), 121–126. https://doi.org/10.1002/cjce.5450750119.

(57) Nilsson, M.; Ingemarsson, Å.; Pedersen, J. R.; Olsson, J. O. Slow Pyrolysis of Birch (Betula) Studied with GC/MS and GC/FTIR/FID. *Chemosphere* **1999**, *38* (7), 1469–1479.

(58) Bierenstiel, M.; Young, T.; Snow, K. Maskwi'omin: A Birch Bark Antibiotic. *Green Teacher* **2018**, 3–7.

(59) O'Donnell, L.; Walsh, A.; Bierenstiel, M.; Taylor, C.; Kuhnke, J. L. Maskwio'mi (Birch Bark Extract): A Case Study Exploring The Use Of A Traditional L'nu Medicine On Skin Conditions. *Wound Care Can.* **2024**, *5* (1). https://doi.org/10.56885/JYTR7825.

(60) Beale, D. J.; Pinu, F. R.; Kouremenos, K. A.; Poojary, M. M.; Narayana, V. K.; Boughton, B. A.; Kanojia, K.; Dayalan, S.; Jones, O. A. H.; Dias, D. A. Review of Recent Developments in GC–MS Approaches to Metabolomics-Based Research. *Metabolomics* **2018**, *14* (11), 152. https://doi.org/10.1007/s11306-018-1449-2.

(61) Staš, M.; Kubička, D.; Chudoba, J.; Pospíšil, M. Overview of Analytical Methods Used for Chemical Characterization of Pyrolysis Bio-Oil. *Energy Fuels* **2014**, *28* (1), 385–402. https://doi.org/10.1021/ef402047y.

(62) Saucier, C.; Polidoro, A. D. S.; Dos Santos, A. L.; Schneider, J. K.; Caramão, E. B.; Jacques, R. A. Comprehensive Two-Dimensional Gas Chromatography with Mass Spectrometry Applied to the Analysis of Volatiles in Artichoke (Cynara Scolymus L.) Leaves. *Ind. Crops Prod.* **2014**, *62*, 507–514. https://doi.org/10.1016/j.indcrop.2014.09.023.

(63) Fancy, S.-A.; Rumpel, K. GC-MS-Based Metabolomics. In *Biomarker Methods in Drug Discovery and Development*; Wang, F., Ed.; Kang, Y. J., Series Ed.; Methods in Pharmacology and Toxicology™; Humana Press: Totowa, NJ, 2008; pp 317–340. https://doi.org/10.1007/978-1-59745-463-6_15.

(64) Ingram, L.; Mohan, D.; Bricka, M.; Steele, P.; Strobel, D.; Crocker, D.; Mitchell, B.; Mohammad, J.; Cantrell, K.; Pittman, C. U. Pyrolysis of Wood and Bark in an Auger Reactor: Physical Properties and Chemical Analysis of the Produced Bio-Oils. *Energy Fuels* **2008**, *22* (1), 614–625. https://doi.org/10.1021/ef700335k.

(65) Cheng, T.; Han, Y.; Zhang, Y.; Xu, C. Molecular Composition of Oxygenated Compounds in Fast Pyrolysis Bio-Oil and Its Supercritical Fluid Extracts. *Fuel* **2016**, *172*, 49–57. https://doi.org/10.1016/j.fuel.2015.12.075.

(66) Tessarolo, N. S.; Dos Santos, L. R. M.; Silva, R. S. F.; Azevedo, D. A. Chemical Characterization of Bio-Oils Using Comprehensive Two-Dimensional Gas Chromatography with Time-of-Flight Mass Spectrometry. *J. Chromatogr. A* **2013**, *1279*, 68–75. https://doi.org/10.1016/j.chroma.2012.12.052.

(67) Schneider, J. K.; Da Cunha, M. E.; Dos Santos, A. L.; Maciel, G. P. S.; Brasil, M. C.; Pinho, A. R.; Mendes, F. L.; Jacques, R. A.; Caramão, E. B. Comprehensive Two Dimensional Gas Chromatography with Fast-Quadrupole Mass Spectrometry

Detector Analysis of Polar Compounds Extracted from the Bio-Oil from the Pyrolysis of Sawdust. *J. Chromatogr. A* **2014**, *1356*, 236–240. https://doi.org/10.1016/j.chroma.2014.06.053.

(68) Joseph, J.; Rasmussen, M. J.; Fecteau, J. P.; Kim, S.; Lee, H.; Tracy, K. A.; Jensen, B. L.; Frederick, B. G.; Stemmler, E. A. Compositional Changes to Low Water Content Bio-Oils during Aging: An NMR, GC/MS, and LC/MS Study. *Energy Fuels* **2016**, *30* (6), 4825–4840. https://doi.org/10.1021/acs.energyfuels.6b00238.

(69) Dos Santos, A.; Lucas, A. N.; Da Mota, I.; Schneider, J.; Polidoro, A.; Pinho, A.; Mendes, F.; Caramão, E. Quantitative GC-MS Analysis of Sawdust Bio-Oil. *J. Braz. Chem. Soc.* **2023**. https://doi.org/10.21577/0103-5053.20230060.

(70) Branca, C.; Giudicianni, P.; Di Blasi, C. GC/MS Characterization of Liquids Generated from Low-Temperature Pyrolysis of Wood. *Ind. Eng. Chem. Res.* **2003**, *42* (14), 3190–3202. https://doi.org/10.1021/ie030066d.

(71) Lu, Y.; Wei, X.-Y.; Cao, J.-P.; Li, P.; Liu, F.-J.; Zhao, Y.-P.; Fan, X.; Zhao, W.; Rong, L.-C.; Wei, Y.-B.; Wang, S.-Z.; Zhou, J.; Zong, Z.-M. Characterization of a Bio-Oil from Pyrolysis of Rice Husk by Detailed Compositional Analysis and Structural Investigation of Lignin. *Bioresour. Technol.* **2012**, *116*, 114–119. https://doi.org/10.1016/j.biortech.2012.04.006.

(72) Moraes, M. S. A.; Migliorini, M. V.; Damasceno, F. C.; Georges, F.; Almeida, S.; Zini, C. A.; Jacques, R. A.; Caramão, E. B. Qualitative Analysis of Bio Oils of Agricultural Residues Obtained through Pyrolysis Using Comprehensive Two Dimensional Gas Chromatography with Time-of-Flight Mass Spectrometric

Detector. *J. Anal. Appl. Pyrolysis* **2012**, *98*, 51–64. https://doi.org/10.1016/j.jaap.2012.05.007.

(73) Rockwood, A. L.; Kushnir, M. M.; Clarke, N. J. Mass Spectrometry. In *Principles and Applications of Clinical Mass Spectrometry*; Elsevier, 2018; pp 33–65. https://doi.org/10.1016/B978-0-12-816063-3.00002-5.

(74) Antony Joseph, M. Transmission Characteristics of the Quadrupole Mass Spectrometer. **2018**. https://doi.org/10.17638/03027712.

(75) Alsbou, E.; Helleur, R. Whole Sample Analysis of Bio-Oils and Thermal Cracking Fractions by Py-GC/MS and TLC–FID. *J. Anal. Appl. Pyrolysis* **2013**, *101*, 222–231. https://doi.org/10.1016/j.jaap.2013.01.003.

(76) Scholze, B.; Meier, D. Characterization of the Water-Insoluble Fraction from Pyrolysis Oil (Pyrolytic Lignin). Part I. PY–GC/MS, FTIR, and Functional Groups. *J. Anal. Appl. Pyrolysis* **2001**, *60* (1), 41–54. https://doi.org/10.1016/S0165-2370(00)00110-8.

(77) Jiang, G.; Nowakowski, D. J.; Bridgwater, A. V. Effect of the Temperature on the Composition of Lignin Pyrolysis Products. *Energy Fuels* **2010**, *24* (8), 4470–4475. https://doi.org/10.1021/ef100363c.

(78) Yildiz, G.; Ronsse, F.; Vercruysse, J.; Daels, J.; Toraman, H. E.; Van Geem, K. M.; Marin, G. B.; Van Duren, R.; Prins, W. In Situ Performance of Various Metal Doped Catalysts in Micro-Pyrolysis and Continuous Fast Pyrolysis. *Fuel Process. Technol.* **2016**, *144*, 312–322. https://doi.org/10.1016/j.fuproc.2016.01.012.

(79) Rapoo, M. T.; Singh, S.; Chong, K.; Banks, S.; Blanco Sanchez, P. H. Analytical Fast Pyrolysis of P. Juliflora: A Thermal and Catalytic Study. *J. Anal. Appl. Pyrolysis* **2023**, *176*, 106254. https://doi.org/10.1016/j.jaap.2023.106254.

(80) Da Cunha, M. E.; Schneider, J. K.; Brasil, M. C.; Cardoso, C. A.; Monteiro, L. R.; Mendes, F. L.; Pinho, A.; Jacques, R. A.; Machado, M. E.; Freitas, L. S.; Caramão, E. B. Analysis of Fractions and Bio-Oil of Sugar Cane Straw by One-Dimensional and Two-Dimensional Gas Chromatography with Quadrupole Mass Spectrometry (GC×GC/qMS). *Microchem. J.* **2013**, *110*, 113–119. https://doi.org/10.1016/j.microc.2013.03.004.

(81) Lievens, C.; Mourant, D.; He, M.; Gunawan, R.; Li, X.; Li, C.-Z. An FT-IR Spectroscopic Study of Carbonyl Functionalities in Bio-Oils. *Fuel* **2011**, *90* (11), 3417–3423. https://doi.org/10.1016/j.fuel.2011.06.001.

(82) Bélanger, J. M. R.; Jocelyn Paré, J. R.; Sigouin, M. Chapter 2 High Performance Liquid Chromatography (HPLC): Principles and Applications. In *Techniques and Instrumentation in Analytical Chemistry*; Elsevier, 1997; Vol. 18, pp 37–59. https://doi.org/10.1016/S0167-9244(97)80011-X.

(83) Undri, A.; Abou-Zaid, M.; Briens, C.; Berruti, F.; Rosi, L.; Bartoli, M.; Frediani, M.; Frediani, P. A Simple Procedure for Chromatographic Analysis of Bio-Oils from Pyrolysis. *J. Anal. Appl. Pyrolysis* **2015**, *114*, 208–221. https://doi.org/10.1016/j.jaap.2015.05.019.

(84) Meile, K.; Zhurinsh, A.; Viksna, A. Comparison of Photodiode Array, Evaporative Light Scattering, and Single-Quadrupole Mass Spectrometric Detection Methods for

the UPLC Analysis of Pyrolysis Liquids. *J. Liq. Chromatogr. Relat. Technol.* **2017**, *40* (7), 369–375. https://doi.org/10.1080/10826076.2017.1308378.

(85) Undri, A.; Abou-Zaid, M.; Briens, C.; Berruti, F.; Rosi, L.; Bartoli, M.; Frediani, M.; Frediani, P. Bio-Oil from Pyrolysis of Wood Pellets Using a Microwave Multimode Oven and Different Microwave Absorbers. *Fuel* **2015**, *153*, 464–482. https://doi.org/10.1016/j.fuel.2015.02.081.

(86) Reymond, C.; Dubuis, A.; Le Masle, A.; Colas, C.; Chahen, L.; Destandau, E.; Charon, N. Characterization of Liquid–Liquid Extraction Fractions from Lignocellulosic Biomass by High Performance Liquid Chromatography Hyphenated to Tandem High-Resolution Mass Spectrometry. *J. Chromatogr. A* **2020**, *1610*, 460569. https://doi.org/10.1016/j.chroma.2019.460569.

(87) Hertkorn, N.; Frommberger, M.; Witt, M.; Koch, B. P.; Schmitt-Kopplin, Ph.; Perdue, E. M. Natural Organic Matter and the Event Horizon of Mass Spectrometry. *Anal. Chem.* **2008**, *80* (23), 8908–8919. https://doi.org/10.1021/ac800464g.

(88) Banerjee, S.; Mazumdar, S. Electrospray Ionization Mass Spectrometry: A Technique to Access the Information beyond the Molecular Weight of the Analyte. *Int. J. Anal. Chem.* **2012**, *2012*, 1–40. https://doi.org/10.1155/2012/282574.

(89) Liu, P.; Xu, C.; Shi, Q.; Pan, N.; Zhang, Y.; Zhao, S.; Chung, K. H. Characterization of Sulfide Compounds in Petroleum: Selective Oxidation Followed by Positive-Ion Electrospray Fourier Transform Ion Cyclotron Resonance Mass Spectrometry. *Anal. Chem.* **2010**, *82* (15), 6601–6606. https://doi.org/10.1021/ac1010553.

(90) Lee, Young Jin. Petroleomic Characterization of Bio-Oil Aging Using Fourier-Transform Ion Cyclotron Resonance Mass Spectrometry. *Bull. Korean Chem. Soc.* **2014**, *35* (3), 811–814. https://doi.org/10.5012/BKCS.2014.35.3.811.

(91) Hertzog, J.; Carré, V.; Le Brech, Y.; Dufour, A.; Aubriet, F. Toward Controlled Ionization Conditions for ESI-FT-ICR-MS Analysis of Bio-Oils from Lignocellulosic Material. *Energy Fuels* **2016**, *30* (7), 5729–5739. https://doi.org/10.1021/acs.energyfuels.6b00655.

(92) Smith, E. A.; Park, S.; Klein, A. T.; Lee, Y. J. Bio-Oil Analysis Using Negative Electrospray Ionization: Comparative Study of High-Resolution Mass Spectrometers and Phenolic versus Sugaric Components. *Energy Fuels* **2012**, *26* (6), 3796–3802. https://doi.org/10.1021/ef3003558.

(93) Desfontaine, V.; Veuthey, J.-L.; Guillarme, D. Hyphenated Detectors. In *Supercritical Fluid Chromatography*; Elsevier, 2017; pp 213–244. https://doi.org/10.1016/B978-0-12-809207-1.00008-2.

(94) Somogyi, Á. Mass Spectrometry Instrumentation and Techniques. In *Medical Applications of Mass Spectrometry*; Elsevier, 2008; pp 93–140. https://doi.org/10.1016/B978-044451980-1.50008-2.

(95) Feith, A.; Teleki, A.; Graf, M.; Favilli, L.; Takors, R. HILIC-Enabled 13C Metabolomics Strategies: Comparing Quantitative Precision and Spectral Accuracy of QTOF High- and QQQ Low-Resolution Mass Spectrometry. *Metabolites* **2019**, *9* (4), 63. https://doi.org/10.3390/metabo9040063.

(96) Chernushevich, I. V.; Loboda, A. V.; Thomson, B. A. An Introduction to Quadrupole–Time-of-flight Mass Spectrometry. *J. Mass Spectrom.* **2001**, *36* (8), 849–865. https://doi.org/10.1002/jms.207.

(97) Wang, Y.; Han, Y.; Hu, W.; Fu, D.; Wang, G. Analytical Strategies for Chemical Characterization of Bio-oil. *J. Sep. Sci.* **2020**, *43* (1), 360–371. https://doi.org/10.1002/jssc.201901014.

(98) Abdelnur, P. V.; Vaz, B. G.; Rocha, J. D.; De Almeida, M. B. B.; Teixeira, M. A. G.; Pereira, R. C. L. Characterization of Bio-Oils from Different Pyrolysis Process Steps and Biomass Using High-Resolution Mass Spectrometry. *Energy Fuels* **2013**, *27* (11), 6646–6654. https://doi.org/10.1021/ef400788v.

(99) Duan, W.; Meng, F.; Cui, H.; Lin, Y.; Wang, G.; Wu, J. Ecotoxicity of Phenol and Cresols to Aquatic Organisms: A Review. *Ecotoxicol. Environ. Saf.* **2018**, *157*, 441–456. https://doi.org/10.1016/j.ecoenv.2018.03.089.

(100) Act, C. A.; Act, R.; Act, R. Environmental Protection Agency (EPA). *Rep. Carcinog.* **2006**, *168*.

(101) American Conference of Governmental Industrial Hygienists. Threshold Limit Values for Chemical Substances and Physical Agents and Biological Exposure Indices; American Conference of Governmental Industrial Hygienists, 2005.

(102) Humans, I. W. G. on the E. of C. R. to; others. Overall Evaluations of Carcinogenicity to Humans: As Evaluated in IARC Monographs Volumes 1-88 (a Total of 900 Agents, Mixtures and Exposures). *Lyon Fr. Cent. Int. Rech. Sur Cancer Monogr. IARC Sur Lévaluation Risques Cancérogènes Pour Homme* **2004**.

(103) Ramalho, M. B.; Durães, A. F. S.; Silvério, F. O.; Pinho, G. P. Determination of Three Cresol Isomers in Sewage Sludge by Solid-Liquid Extraction with Low Temperature Purification and Gas Chromatography-Mass Spectrometry. *J. Environ. Sci. Health Part B* **2020**, *55* (3), 184–192. https://doi.org/10.1080/03601234.2019.1678952.

(104) Schettgen, T.; Alt, A.; Dewes, P.; Kraus, T. Simple and Sensitive GC/MS-Method for the Quantification of Urinary Phenol, o- and m-Cresol and Ethylphenols as Biomarkers of Exposure to Industrial Solvents. *J. Chromatogr. B* **2015**, *995–996*, 93–100. https://doi.org/10.1016/j.jchromb.2015.05.023.

(105) Schummer, C.; Delhomme, O.; Appenzeller, B.; Wennig, R.; Millet, M. Comparison of MTBSTFA and BSTFA in Derivatization Reactions of Polar Compounds Prior to GC/MS Analysis. *Talanta* **2009**, *77* (4), 1473–1482. https://doi.org/10.1016/j.talanta.2008.09.043.

(106) Martín-Pozo, L.; Arena, K.; Cacciola, F.; Dugo, P.; Mondello, L. Comprehensive Two-Dimensional Liquid Chromatography in Food Analysis. Is Any Sample Preparation Necessary? *Green Anal. Chem.* **2022**, *3*, 100025. https://doi.org/10.1016/j.greeac.2022.100025.

(107) Ruas, M. E. A.; Silvério, F. O.; Pinho, G. P. Development of a Low-Temperature Purification Method for Gas Chromatography–Mass Spectrometry Quantification of Three Cresol Isomers in Smoked Bacon. *Food Anal. Methods* **2024**. https://doi.org/10.1007/s12161-024-02687-6.

(108) Lyczywek, V.; Kaliaperumal, R.; Zuieva, V.; Titcombe, S.; Bierenstiel, M. Qualitative and Quantitative Analysis of Cresols Found in Maskwio'mi (Birch Bark

Extract). *Can. J. Chem.* **2024**, *102* (4), 289–295. https://doi.org/10.1139/cjc-2023-0166.

(109) Haynes, W.M. *CRC Handbook of Chemistry and Physics.*; 95th Edition.; CRC Press LLC, Boca Raton: FL, 2014.

(110) Calvo, E.; Camafeita, E.; Fernández-Gutiérrez, B.; López, J. A. Applying Selected Reaction Monitoring to Targeted Proteomics. *Expert Rev. Proteomics* **2011**, *8* (2), 165–173. https://doi.org/10.1586/epr.11.11.

(111) Sherman, J.; McKay, M. J.; Ashman, K.; Molloy, M. P. How Specific Is My SRM?: The Issue of Precursor and Product Ion Redundancy. *PROTEOMICS* **2009**, *9* (5), 1120–1123. https://doi.org/10.1002/pmic.200800577.

(112) Holman, S. W.; Sims, P. F. G.; Eyers, C. E. The Use of Selected Reaction Monitoring in Quantitative Proteomics. *Bioanalysis* **2012**, *4* (14), 1763–1786. https://doi.org/10.4155/bio.12.126.

(113) Rhourri-Frih, B.; Chaimbault, P.; Claude, B.; Lamy, C.; André, P.; Lafosse, M. Analysis of Pentacyclic Triterpenes by LC–MS. A Comparative Study between APCI and APPI. *J. Mass Spectrom.* **2009**, *44* (1), 71–80. https://doi.org/10.1002/jms.1472.

(114) Gobo, L. A.; Viana, C.; Lameira, O. A.; De Carvalho, L. M. A Liquid Chromatography-Atmospheric Pressure Photoionization Tandem Mass Spectrometric (LC-APPI-MS/MS) Method for the Determination of Triterpenoids in Medicinal Plant Extracts: LC-APPI-MS/MS for Determination of Triterpenoids. *J. Mass Spectrom.* **2016**, *51* (8), 558–565. https://doi.org/10.1002/jms.3783.

(115) Kosyakov, D. S.; Ul'yanovskii, N. V.; Falev, D. I. Determination of Triterpenoids from Birch Bark by Liquid Chromatography-Tandem Mass Spectrometry. *J. Anal. Chem.* **2014**, *69* (13), 1264–1269. https://doi.org/10.1134/S1061934814130061.

(116) Mishra, T.; Chandra, P.; Kumar, B.; Baleshwar, M.; Joshi, P.; Rana, T. S.; Upreti, D. K.; Pal, M. Phytochemical Profiling of the Stem Bark of *Betula Utilis* from Different Geographical Regions of India Using UHPLC-ESI-MS/MS. *Anal. Sci. Adv.* **2021**, *2* (11–12), 497–504. https://doi.org/10.1002/ansa.202000073.

(117) Mase, C.; Sueur, M.; Lavanant, H.; Rüger, C. P.; Giusti, P.; Afonso, C. Ion Source Complementarity for Characterization of Complex Organic Mixtures Using Fourier Transform Mass Spectrometry: A Review. *Mass Spectrom. Rev.* **2024**, mas.21910. https://doi.org/10.1002/mas.21910.

(118) Burnouf-Radosevich, M.; Delfel, N. E.; England, R. Gas Chromatography-Mass Spectrometry of Oleanane- and Ursane-Type Triterpenes—Application to Chenopodium Quinoa Triterpenes. *Phytochemistry* **1985**, *24* (9), 2063–2066. https://doi.org/10.1016/S0031-9422(00)83122-2.

(119) Santos, P.; Gomes, L.; Mazzei, J.; Fontão, A. P.; Sampaio, A.; Siani, A.; Valente, L. POLYPHENOL AND TRITERPENOID CONSTITUENTS OF Eugenia Florida DC. (MYRTACEAE) LEAVES AND THEIR ANTIOXIDANT AND CYTOTOXIC POTENTIAL. *Quím. Nova* **2018**. https://doi.org/10.21577/0100-4042.20170284.